Electronic Supplementary Material (ESI) for Dalton Transactions.
This journal is © The Royal Society of Chemistry 2019

Cytotoxic Ru^{II}-*p*-cymene complexes of an anthraimidazoledione: halide dependent solution stability, reactivity and resistance to hypoxia deactivation

Amrita Sarkar‡, Sourav Acharya‡, Kumar Khushvant, Kallol Purkait and Arindam Mukherjee*

Department of Chemical Sciences, Indian Institute of Science Education and Research Kolkata,

Mohanpur campus - 741246, India.

Corresponding author. Fax: (+91)033-25873118; Tel: (+91)033-25873121;

E-mail: a.mukherjee@iiserkol.ac.in

‡ both the authors contributed equally

Contents

1. Molecular docking 7

Fig. S1 ^{1}H NMR of ligand PAIDH in $CDCl_3$, 400 MHz. Inset shows aromatic region where corresponding protons are designated accordingly. 8

Fig. S2 ^{1}H NMR of complex **1** in DMSO-d_6, 500 MHz. 8

Fig. S3 ^{13}C NMR of complex **1** in DMSO-d_6, 125 MHz. 9

Fig. S4 ^{13}C DEPT-135 NMR of complex **1** in DMSO-d_6 9

Fig. S5 HMQC spectra of complex **1** in DMSO-d_6. 10

Fig. S6 ^{1}H NMR of complex **2** in DMSO-d_6, 500 MHz. 10

Fig. S7 ^{13}C NMR of complex **2** in DMSO-d_6, 125 MHz. 11

Fig. S8 ^{13}C DEPT-135 NMR of complex **2** in DMSO-d_6 11

Fig. S9 HMQC of complex **2** in DMSO-d_6. 12

Fig. S10 ^{1}H NMR of complex **3** in DMSO-d_6, 500 MHz. 12

Fig. S11 ^{13}C NMR of complex **3** in DMSO-d_6, 125 MHz. 13

Fig. S12 ^{13}C DEPT-135 NMR of complex **3** in DMSO-d_6 13

Fig. S13 HMQC of complex **3** in DMSO-d_6. 14

Fig. S14 UV-Vis spectra of complex **1-3** (A, B and C respectively) in DMF. UV region peaks (For **1:** 280 & 386, **2:** 274 & 372, **3:** 284 & 371 nm) can be attributed as π to π* transitions of the ligand PAIDH. Visible region peak is for MLCT transitions metal d(π) orbital to vacant π* orbital of ligand PAIDH. 14

Fig. S15 ^{1}H NMR kinetic experiments to study hydrolysis of complex **1** in PBS buffer solution (pH = 7.4) in presence of 110 mM NaCl. No hydrolysis peak as well as arene loss peak is observed during the experiment for 3 days. 15

Fig. S16 ^{1}H NMR kinetic experiments to study hydrolysis of complex **1** in PBS buffer solution (pH = 7.4) in presence of 4 mM NaCl. '*' denotes the hydrolyzed peaks and '#' stands for the peak for arene after loss from the metal center 15

Fig. S17 ESI-MS spectra of hydrolysis study of complex **1** incubated with 2:8 *v/v* methanol and 10 mM phosphate buffer (pH 7.4) with 4 mM NaCl, recorded after 0.5 h. Spectra represents experimental and simulated *m/z* values along with isotopic resolution of monocationic complexes- (A) **1** without halide, (B) aquated complex & (C) overall speciation with the molecular ion peak in the inset (red border). All the simulated spectra are represented in red colour. PAID = anionic form of the ligand PAIDH. 16

Fig. S18 ESI-MS spectra of hydrolysis study of complex **1** incubated with 2:8 *v/v* methanol and 10 mM phosphate buffer (pH 7.4) with 4 mM NaCl, recorded after 24 h. Spectra represents experimental and simulated *m/z* values along with isotopic resolution of monocationic complexes- (A) **1** without halide, (B) aquated complex & (C) overall speciation with the molecular ion peak in the inset (red border). All the simulated spectra are represented in red colour. PAID = anionic form of the ligand PAIDH. 17

Fig. S19 ^{1}H NMR kinetic experiments to study hydrolysis of complex **2** in PBS buffer solution (pH = 7.4) in presence of 110 mM NaCl. '!' stands for the halide exchange forming **1** in solution. No arene loss is evident during the experiment for 3 days. 18

Fig. S20 ^{1}H NMR kinetic experiments to study hydrolysis of complex **2** in PBS buffer solution (pH = 7.4) in presence of 4 mM NaCl. '**!**' denotes the peaks arising due to halide exchange to form **1**. '*****' denotes the hydrolyzed peaks. 18

Fig. S21 ^{1}H NMR kinetic experiments to study hydrolysis of complex **3** in PBS buffer solution (pH = 7.4) in presence of 110 mM NaCl. '**!**' denotes the peaks arising due to halide exchange to form **1** and '**#**' stands for the peak of arene after loss from the metal center. No hydrolyzed peaks were observed during the course of the experiment for 3 days. 19

Fig. S22 ^{1}H NMR kinetic experiments to study hydrolysis of complex **3** in PBS buffer solution (pH = 7.4) in presence of 4 mM NaCl. '**!**' denotes the peaks arising due to halide exchange leading to formation of **1** and '**#**' stands for the peak of arene after loss from the metal center. No hydrolyzed peaks were observed during the course of the experiment for 3 days. 19

Fig. S23 ESI-MS spectra of hydrolysis study of complex **2** incubated with 2:8 *v/v* methanol and 10 mM phosphate buffer (pH 7.4) with 4 mM NaCl, recorded after 0.5 h. Spectra represents experimental and simulated *m/z* values along with isotopic resolution of monocationic complexes- (A) complex without halide, (B) aquated complex, (C) Chloride exchange forming **1** from **2,** (D) molecular ion peak of **2** and (E) overall speciation. All the simulated spectra are represented in red colour. PAID = anionic form of the ligand PAIDH. 20

Fig. S24 ESI-MS spectra of hydrolysis study of complex **2** incubated with 2:8 *v/v* methanol and 10 mM phosphate buffer (pH 7.4) with 4 mM NaCl, recorded after 24 h. Spectra represents experimental and simulated *m/z* values along with isotopic resolution of monocationic complexes- (A) complex without halide, (B) Chloride exchange forming **1** from **2** and (C) overall speciation with the molecular ion peak in the inset (red border). All the simulated spectra are represented in red colour. PAID = anionic form of the ligand PAIDH. 21

Fig. S25 ESI-MS spectra of hydrolysis study of complex **3** incubated with 2:8 *v/v* methanol and 10 mM phosphate buffer (pH 7.4) with 4 mM NaCl, recorded after 0.5 h. Spectra represents experimental and simulated *m/z* values along with isotopic resolution of monocationic complexes- (A) Chloride exchange forming **1** from **3** in very small amount, (B) molecular ion peak of **3** and (C) overall speciation. All the simulated spectra are represented in red colour..... 22

Fig. S26 ESI-MS spectra of hydrolysis study of complex **3** incubated with 2:8 *v/v* methanol and 10 mM phosphate buffer (pH 7.4) with 4 mM NaCl, recorded after 24 h, shows exchange of halide is much less compared to **2**. Spectra represents experimental and simulated *m/z* values along with isotopic resolution of monocationic complexes- (A) Chloride exchange forming **1** from **3** in very small amount, (B) molecular ion peak of **3** and (C) overall speciation. All the simulated spectra are represented in red colour. PAID = anionic form of the ligand PAIDH. 23

Fig. S27 Stack plot of ^{1}H NMR spectra of reduced L-glutathione (below), complex **1** and reduced L-glutathione (all the three from above) in DMSO-d_6/D_2O 7:3 (*v/v*) mixture, recorded at different interval of time at 25 °C. '**§**' stands for GSH auto-oxidation product, '**$**' GSH bound peaks. 24

Fig. S28 Stack plot of ^{1}H NMR spectra of reduced L-glutathione (below), complex **2** and reduced L-glutathione (all the three from above) in DMSO-d_6/D_2O 7:3 (*v/v*) mixture, recorded at

different interval of time at 25°C. '**§**' stands for GSH auto-oxidation product, '**$**' GSH bound peaks corresponding to both [(PAIDH)Ru^{II}(*p*-cym)(GS)]$^+$ and [Ru^{II}(*p*-cym)(GS)]$^+$. 24

Fig. S29 ESI-MS spectrum of glutathione (GSH) interaction with complex **1** using 1:2.5 mol ratio of complex:GSH. Incubation in 2:8 *v/v* methanol and 4 mM aqueous NaCl, recorded after 2 h. No GSH adduct with **1** was found. 25

Fig. S30 ESI-MS spectrum of GSH interaction with complex **1** using 1:2.5 mole ratio of complex:GSH. Incubation in 2:8 *v/v* methanol and 4 mM aqueous NaCl, recorded after 24 h. The overall peak intensities show that there has been increase in GSH adduct intensity. Spectra represents experimental and simulated *m/z* values along with isotopic resolution of monocationic complexes- (A) PAIDH dissociated GSH bound metal complex, [Ru(GS)(*p*-cym)]$^+$, (B) GSH adduct of halide dissociated complex, [Ru(PAIDH)(GS)(*p*-cym)]$^+$ and (C) overall speciation (inset: sodiated GSH adduct of **1**, [Ru(PAID)(GS)(*p*-cym)]Na^+). All the simulated spectra are represented in red colour. [PAID = anionic form of the ligand PAIDH and GS = anionic glutathione] 26

Fig. S31 ESI-MS spectrum of GSH interaction with complex **2** using 1:2.5 mole ratio of complex:GSH. Incubation in 2:8 *v/v* methanol and 4 mM aqueous NaCl, recorded after 2 h. The overall peak intensities show that there is more GSH adduct than that of **1**. Spectra shows isotopic resolution of monocationic complexes- (A) magnified view showing the halide dissociated **2**, aquated species, chloride exchange forming **1** from **2**, molecular ion peak of **2** and (B) over all speciation (inset: GSH adduct of **2**, [Ru(PAIDH)(GS)(*p*-cym)]$^+$). All the simulated spectra are represented in red colour. [PAID = anionic form of the ligand PAIDH and GS = anionic glutathione] 27

Fig. S32 ESI-MS spectrum of GSH interaction with complex **2** using 1:2.5 mol ratio of complex:GSH. Incubation in 2:8 *v/v* methanol and 4 mM aqueous NaCl, recorded after 24 h. The overall peak intensities show that the most intense is the GSH adduct peak. Spectra shows isotopic resolution of monocationic complexes showing PAIDH dissociated GSH bound metal complex, [Ru(*p*-cym)(GS)]$^+$; the halide dissociated **2**, [Ru(PAID)(*p*-cym)]$^+$; aquated species, [Ru(PAID)(*p*-cym)(H_2O)]$^+$; chloride exchange forming **1** from **2**, [Ru(PAIDH)(*p*-cym)Cl]$^+$; molecular ion peak of **2**, [Ru(PAIDH)(*p*-cym)Br]$^+$; GSH adduct of **2**, [Ru(PAIDH)(GS)(*p*-cym)]$^+$) and [Ru(PAID)(*p*-cym)(GS)]Na^+. [PAID = anionic form of the ligand PAIDH and GS = anionic glutathione] 28

Fig. S33 ESI-MS spectrum of GSH interaction with complex **3** using 1:2.5 mol ratio of complex:GSH. Incubation in 2:8 *v/v* methanol and 4 mM aqueous NaCl, recorded after 2 h. The overall peak intensities show that there is no adduct formation with GSH, unlike complex **2**. ... 29

Fig. S34 ESI-MS spectrum of GSH interaction with complex **3** using 1:2.5 mol ratio of complex:GSH. Incubation in 2:8 *v/v* methanol and 4 mM aqueous NaCl, recorded after 24 h. The overall peak intensities show that there is very small amount of adduct formation with GSH even after 24 h, unlike complex **1** and **2**..... 30

Fig. S35 ESI-MS spectra of 9-ethylguanine(9-EtG) interaction with complex **1** using 1:1 mol ratio of complex:9-EtG. Incubation in 2:8 *v/v* methanol and 4 mM aqueous NaCl, recorded after 2 h, showing 9-EtG bound complex. Spectra represents *m/z* values along with isotopic resolution of monocationic complexes- (A) magnified view showing the halide dissociated **1**, aquated species, molecular ion peak and (B) overall speciation with the 9-EtG bound **1** (inset: magnified

view of the 9-EtG bound species along with the simulation). All the simulated spectra are represented in red colour. PAID = anionic form of the ligand PAIDH. 31

Fig. S36 ESI-MS spectrum of 9-ethylguanine(9-EtG) interaction with complex **1** using 1:1 mol ratio of complex:9-EtG. Incubation in 2:8 *v/v* methanol and 4 mM aqueous NaCl, recorded after 24 h, showing 9-EtG bound complex. The dehalogenated species concentration shows a ratio metric increase over a 24 h period. 32

Fig. S37 ESI-MS spectrum of 9-ethylguanine (9-EtG) interaction with complex **2** using 1:1 mol ratio of complex:9-EtG. Incubation in 2:8 *v/v* methanol and 4 mM aqueous NaCl, recorded after 2 h, showing that the most intense *m/z* corresponds to 9-EtG adduct with **2**. 33

Fig. S38 ESI-MS spectrum of 9-ethylguanine (9-EtG) interaction with complex **2** using 1:1 mol ratio of complex:9-EtG. Incubation in 2:8 *v/v* methanol and 4 mM aqueous NaCl, recorded after 24 h. The overall peak intensities show a decrease suggesting there may be degradation or precipitation of the complex from solution. '¥' stands for uncharacterized polynuclear Ru species. 34

Fig. S39 ESI-MS spectrum of 9-ethylguanine (9-EtG) interaction with complex **3** using 1:1 mol ratio of complex:9-EtG. Incubation in 2:8 *v/v* methanol and 4 mM aqueous NaCl, recorded after 2 h. The overall peak intensities show that there is hardly any adduct formation with 9-EtG. There is some '¥' uncharacterized polynuclear Ru species in the same place where the dehalogenated species appears. 35

Fig. S40 ESI-MS spectrum of 9-ethylguanine (9-EtG) interaction with complex **3** using 1:1 mol ratio of complex:9-EtG. Incubation in 2:8 *v/v* methanol and 4 mM aqueous NaCl, recorded after 24 h. The overall peak intensities show that there is formation of a small amount of adduct with 9-EtG. There is also some '¥' uncharacterized polynuclear Ru species in the same place where the dehalogenated species appears. 36

Fig. S41 9-Ethyl Guanine binding of **3** in DMSO-d_6/D_2O 7:3 (*v/v*) mixture, recorded at different interval of time at 25 °C. Recording started after 5 minutes of dissolving 9-Ethyl guanine and complex **3** together. '**Δ**' stands for the metal complex peaks and '**%**' stands for the 9-Ethyl guanine peaks of the 9-EtG bound metal complex species. 37

Fig. S42 Cytotoxicity of HepG2 cells under normoxic condition in presence of different concentration of N-acetyl cysteine (NAC). Concentration taken from 100 µM to 1 mM. 37

Fig. S43 Plots of cell viability (%) vs. log of concentrations of **1-3** against HepG2 cell line after incubation for 48 h determined from MTT assays under normoxic condition. The plots provided are for one independent experiment (each concentration in triplicate) out of at least three independent experiments. 38

Fig. S44 Plots of cell viability (%) vs. log of concentrations of **1-3** against MIA PaCa-2 cell line after incubation for 48 h determined from MTT assays under normoxic condition. The plots provided are for one independent experiment (each concentration in triplicate) out of at least three independent experiments. 38

Fig. S45 Plots of cell viability (%) vs. log of concentrations of **1-3** against MDA-MB-231 cell line after incubation for 48 h determined from MTT assays under normoxic condition. The plots provided are for one independent experiment (each concentration in triplicate) out of at least three independent experiments. 38

Table S1 Cell cycle analysis of MIA PaCa-2 treated with **1-3**, showing percentage of arrest in different phases of cell cycle..... 39

Fig. S46 EFGR kinase domain (PDB: 1M17) interaction of the clinical EGFR inhibitor Erlotinib (A) vs. the PAIDH ligand (B) using Schrödinger. (C) A representative diagram of both Erlotinib and PAIDH at the active sight cavity of the 1M17 protein showing both of them occupy almost the same site but the PAIDH shows a pi-pi stacking with phenylalanine (Phe 699) from the active. Yellow: PAIDH, Red: Erlotinib. 40

1. Molecular docking

In this work we have chosen Erlotinib bound EGFR protein crystal structure (PDB: 1M17)[1] from Brookhaven Protein Data Bank (RCSB), out of the large number of EGFR crystal structure, to predict the possible modes of binding of the ligand PAIDH. The PDB structure was optimized after removing the bound inhibitor, water and processed by applying the OPLS_2005 force field by the protein preparation utility in Maestro Suite 2016-1 in Maestro (Schrödinger Suite 2016-1 Protein Preparation Wizard; Epik, Schrödinger, LLC, New York, NY, 2016; Impact, Schrödinger, LLC, New York, NY, 2016; Prime, Schrödinger, LLC, New York, NY, 2016).[2] The erlotinib and the optimized ligand PAIDH were then prepared and minimized by means of OPLS_2005.[3-5] The lowest energy conformer in ligprep output was docked in the EGFR tyrosine kinase active site (Coordinates of the site: X = 21.6, Y = 0.24, Z = 52.96) using extra precision (XP) within 10 Å cubic distance. The grid box used in the docking process is large enough to cover the entire active site.

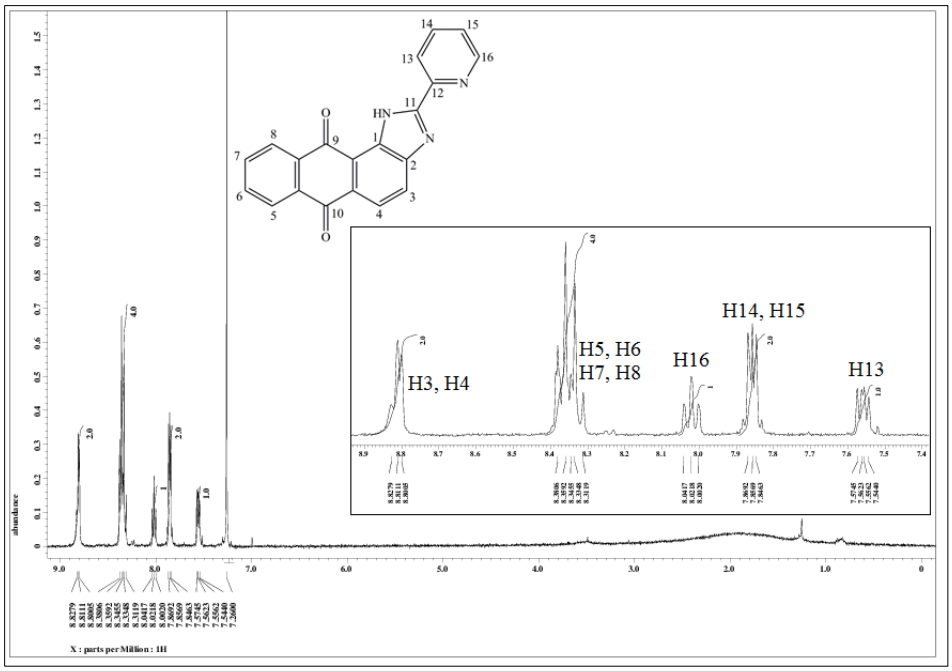

Fig. S1 ^{1}H NMR of ligand PAIDH in $CDCl_3$, 400 MHz. Inset shows aromatic region where corresponding protons are designated accordingly.

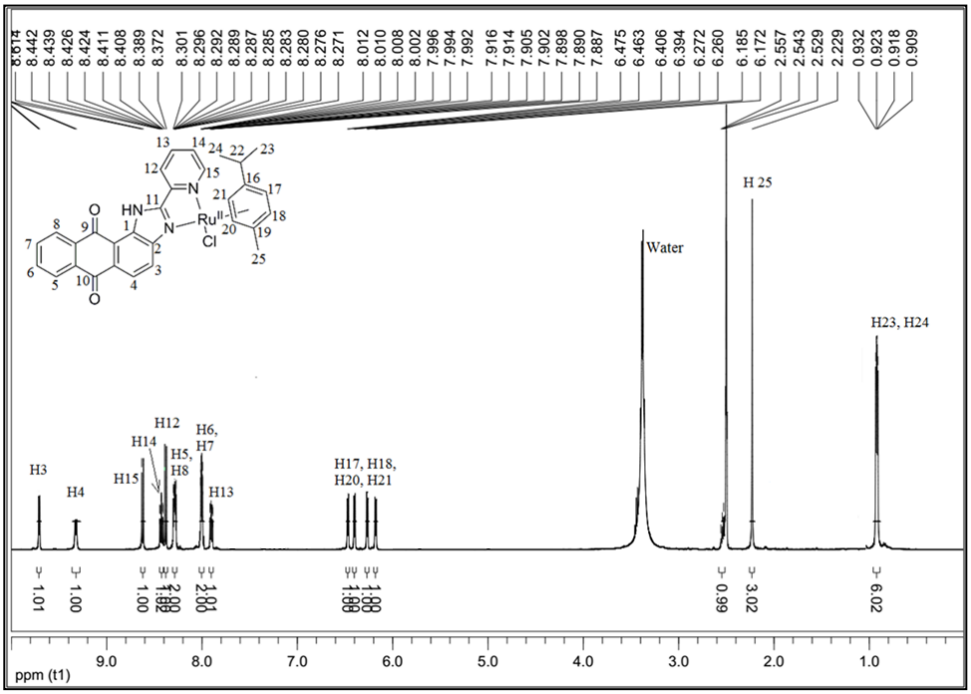

Fig. S2 ^{1}H NMR of complex **1** in DMSO-d_6, 500 MHz.

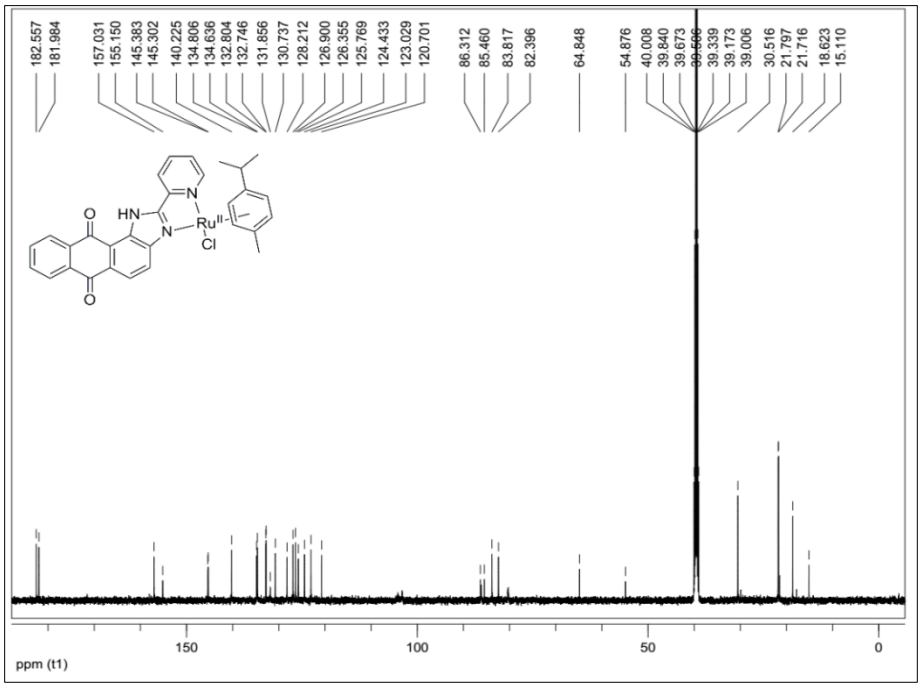

Fig. S3 ^{13}C NMR of complex **1** in DMSO-d_6, 125 MHz.

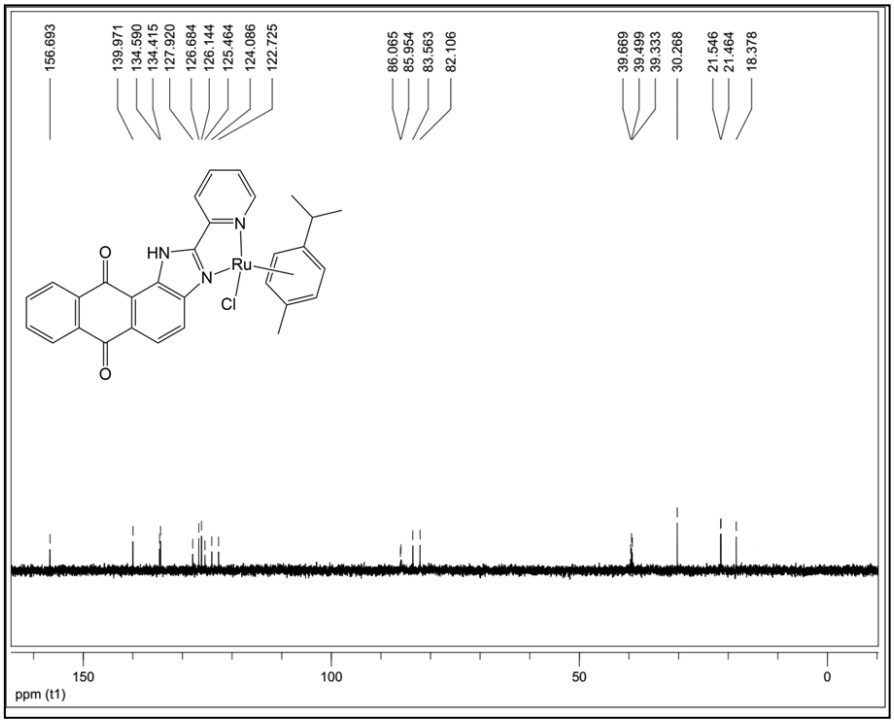

Fig. S4 ^{13}C DEPT-135 NMR of complex **1** in DMSO-d_6.

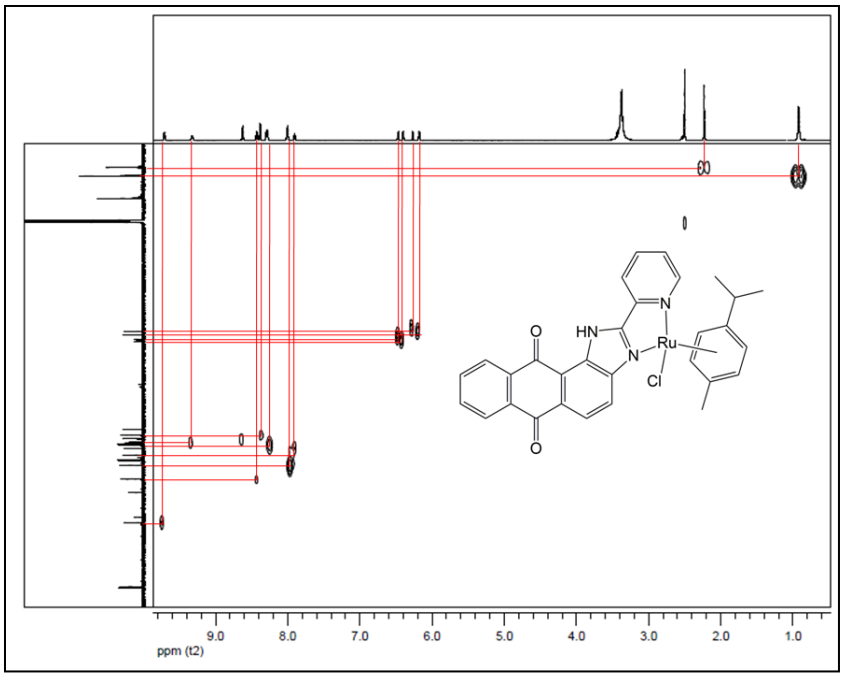

Fig. S5 HMQC spectra of complex **1** in DMSO-d_6.

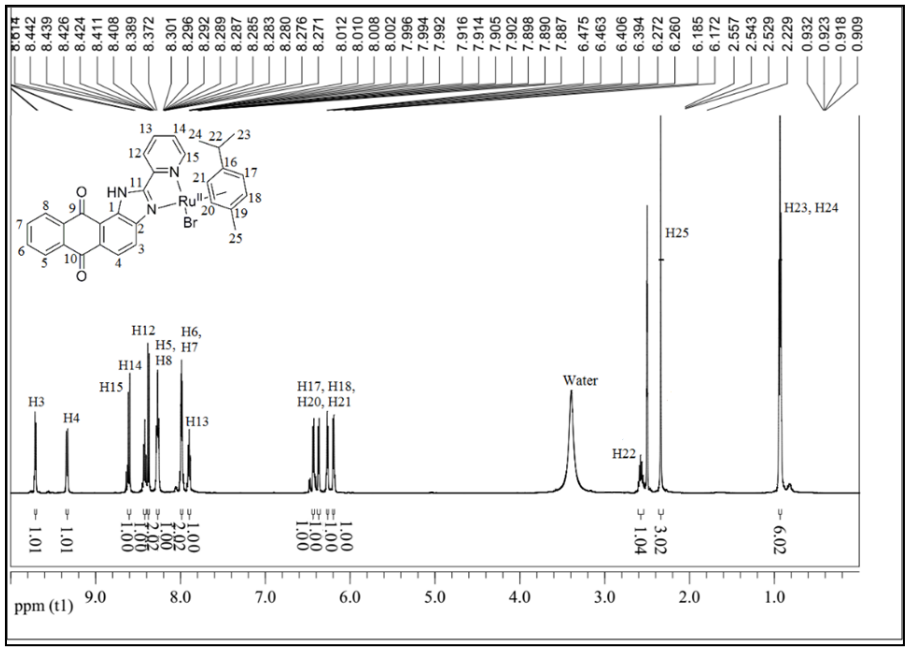

Fig. S6 ^{1}H NMR of complex **2** in DMSO-d_6, 500 MHz.

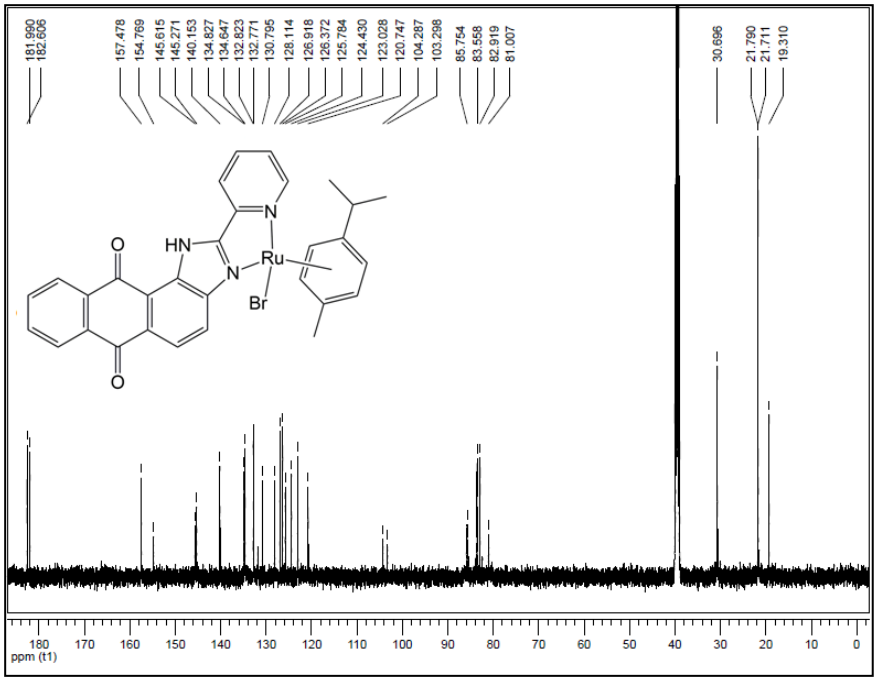

Fig. S7 ^{13}C NMR of complex **2** in DMSO-d_6, 125 MHz.

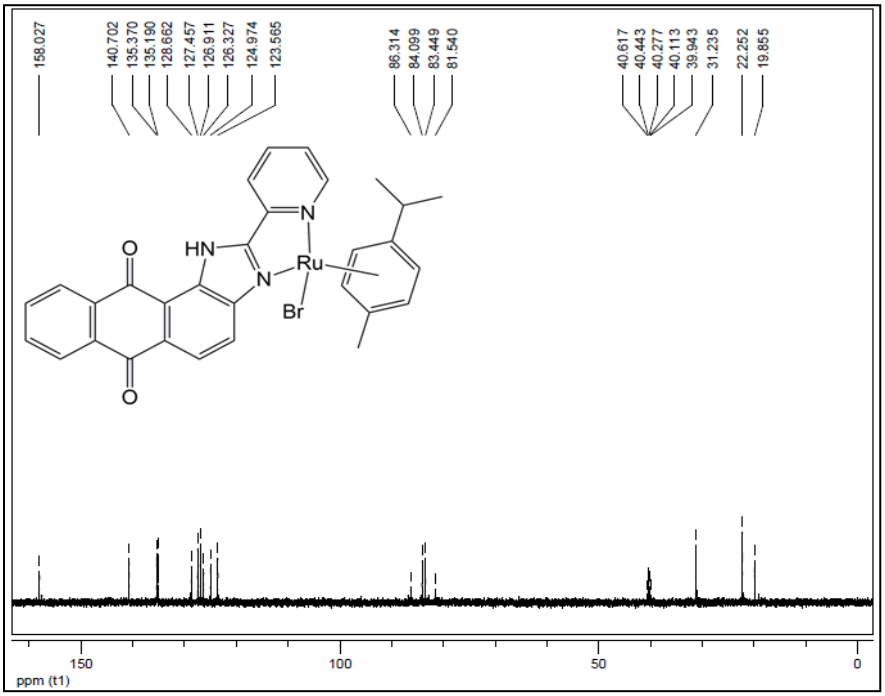

Fig. S8 ^{13}C DEPT-135 NMR of complex **2** in DMSO-d_6.

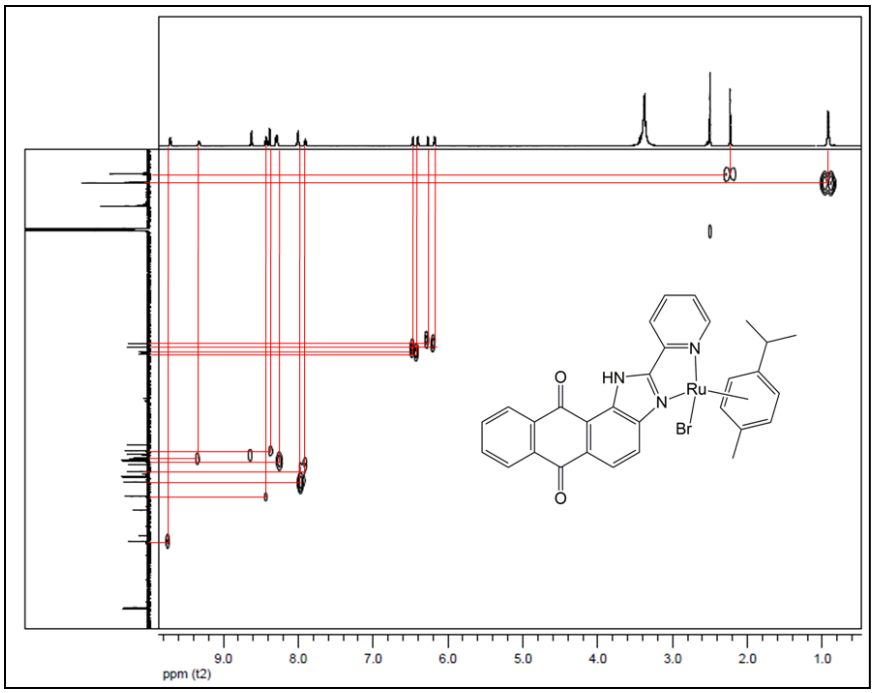

Fig. S9 HMQC of complex **2** in DMSO-d_6.

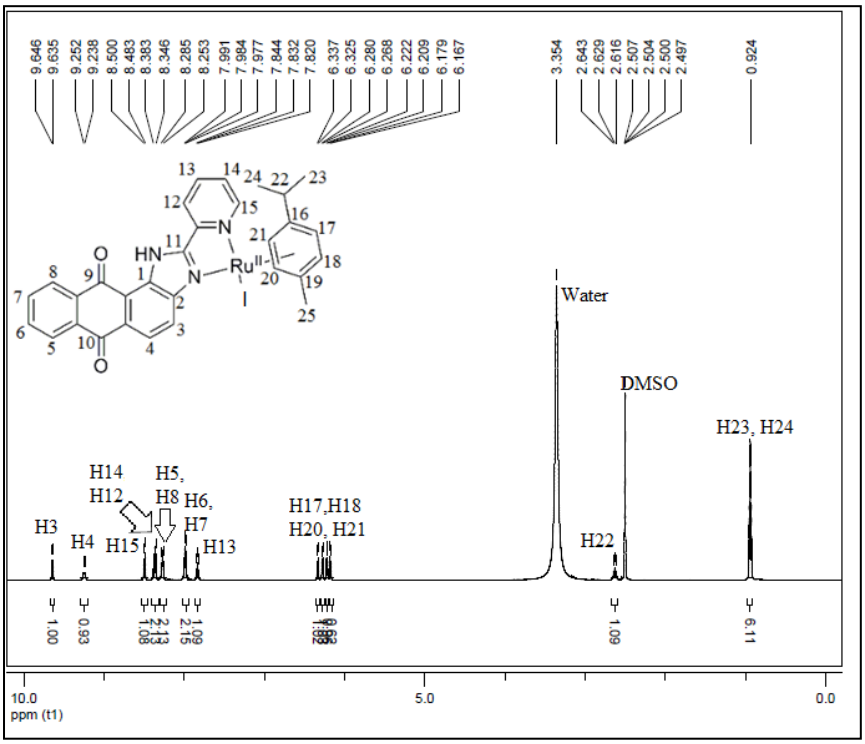

Fig. S10 ^{1}H NMR of complex **3** in DMSO-d_6, 500 MHz.

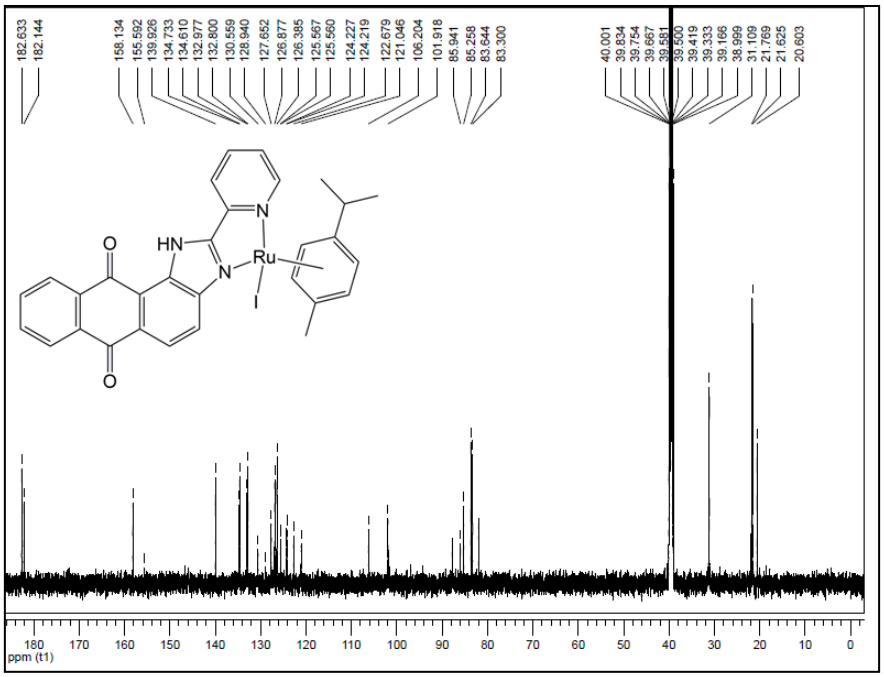

Fig. S11 ^{13}C NMR of complex **3** in DMSO-d_6, 125 MHz.

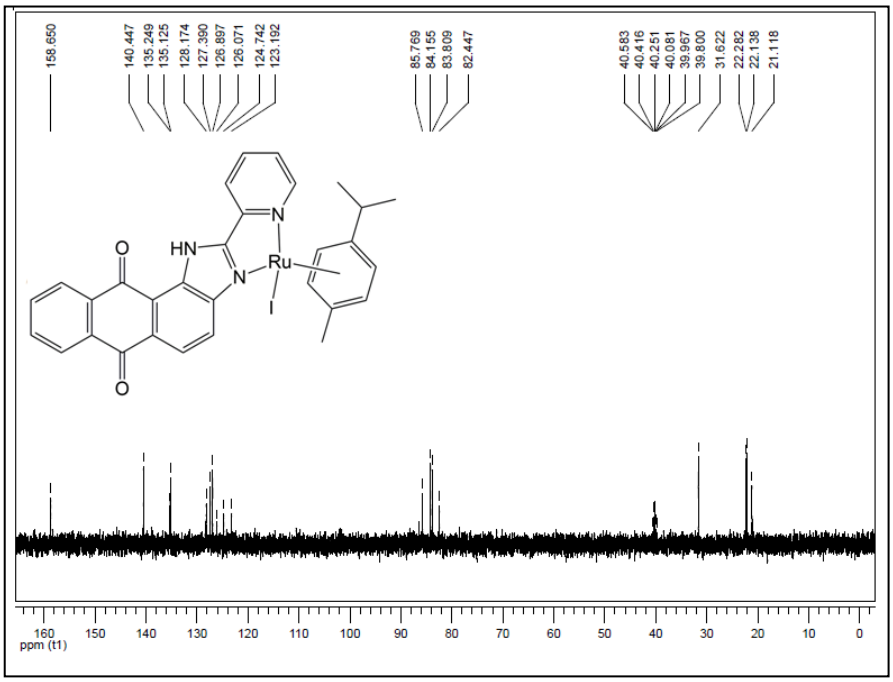

Fig. S12 ^{13}C DEPT-135 NMR of complex **3** in DMSO-d_6.

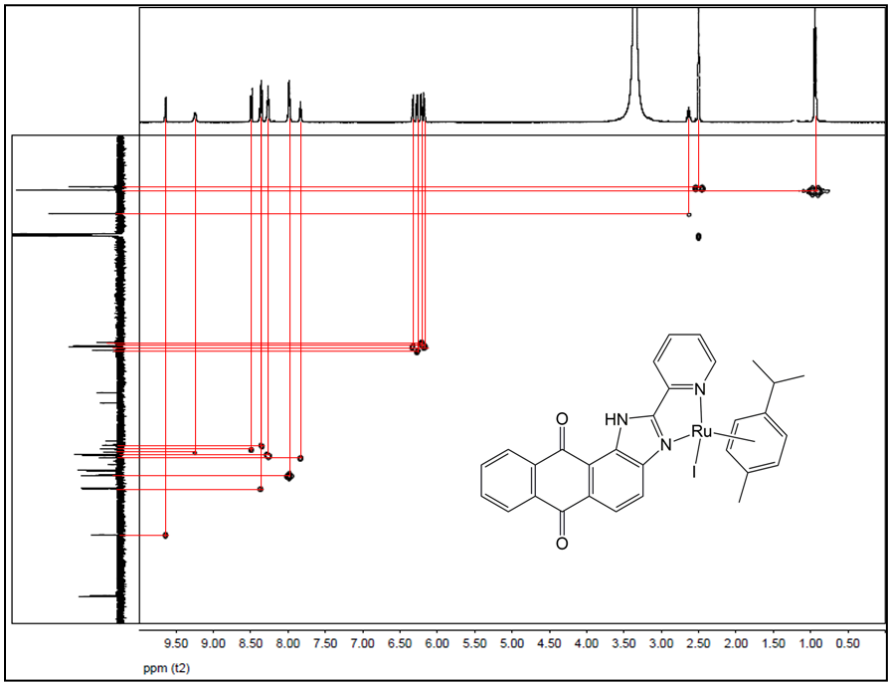

Fig. S13 HMQC of complex **3** in DMSO-d_6.

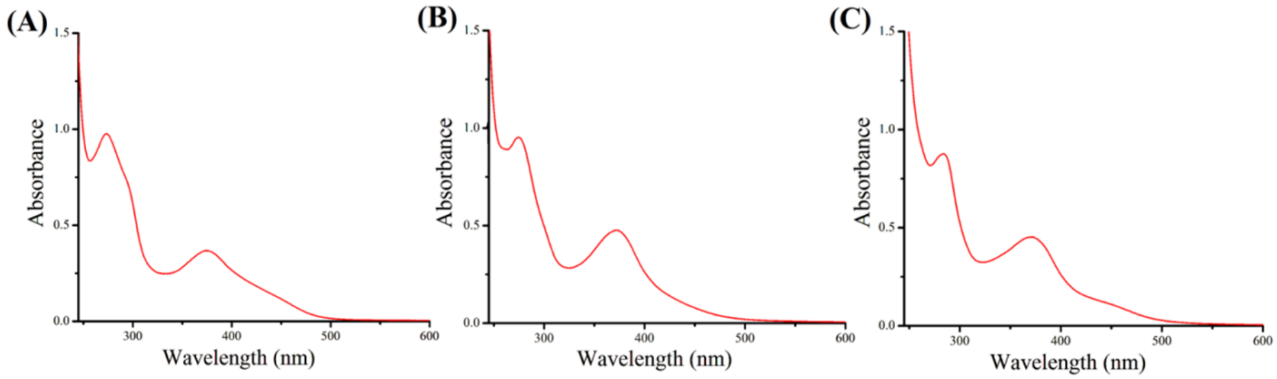

Fig. S14 UV-Vis spectra of complex **1-3** (A, B and C respectively) in DMF. UV region peaks (For **1:** 280 & 386, **2:** 274 & 372, **3:** 284 & 371 nm) can be attributed as π to π* transitions of the ligand PAIDH. Visible region peak is for MLCT transitions metal d(π) orbital to vacant π* orbital of ligand PAIDH.

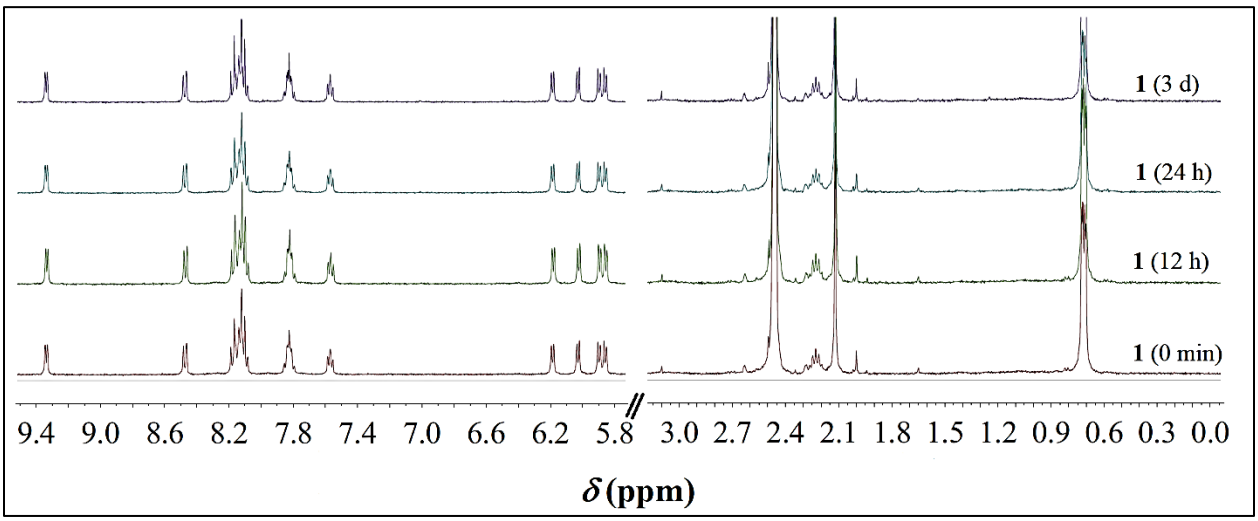

Fig. S15 ^{1}H NMR kinetic experiments to study hydrolysis of complex **1** in PBS buffer solution (pH = 7.4) in presence of 110 mM NaCl. No hydrolysis peak as well as arene loss peak is observed during the experiment for 3 days.

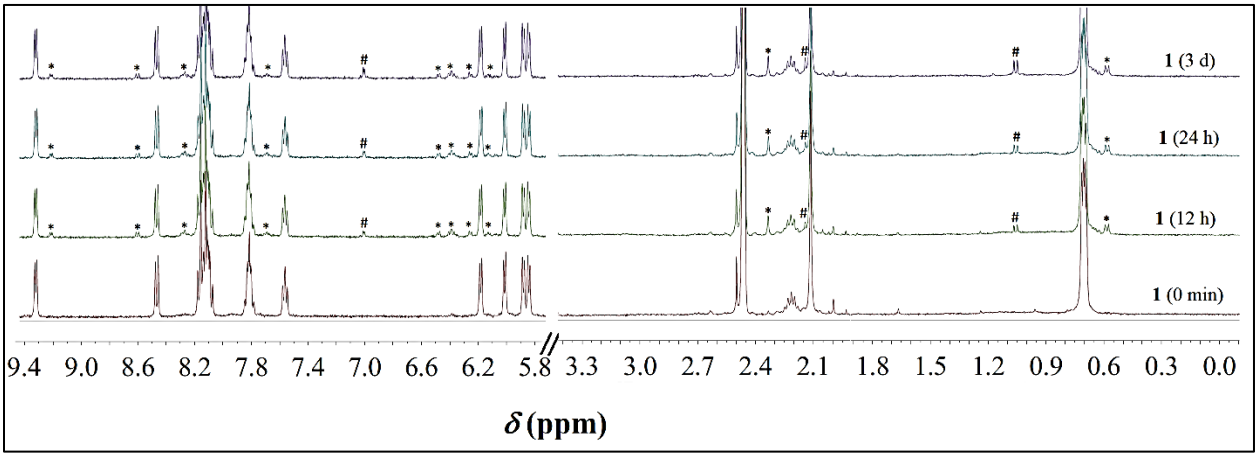

Fig. S16 ^{1}H NMR kinetic experiments to study hydrolysis of complex **1** in PBS buffer solution (pH = 7.4) in presence of 4 mM NaCl. '*' denotes the hydrolyzed peaks and '#' stands for the peak for arene after loss from the metal center.

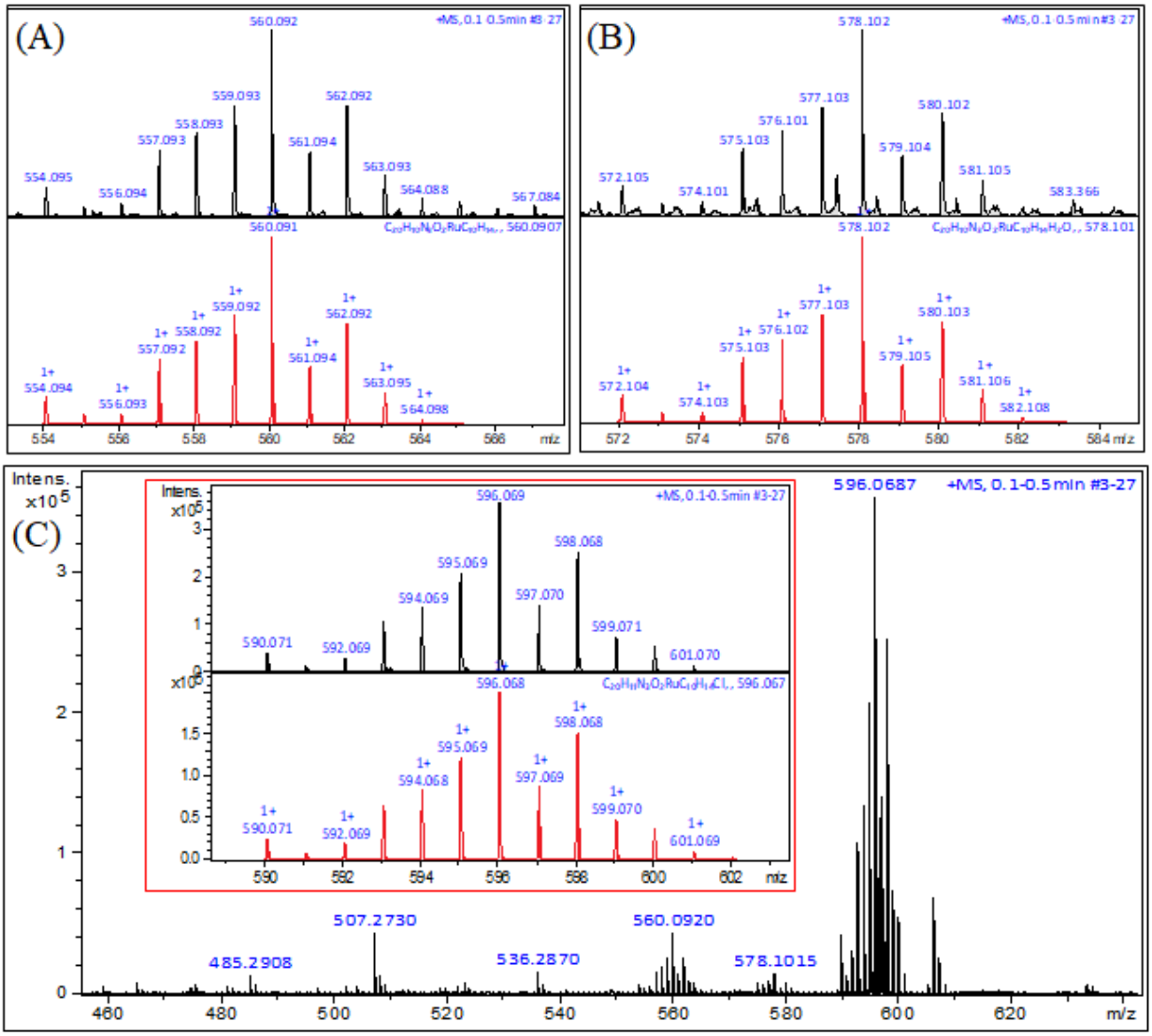

Figure	species	Exp. *m/z*	Calc. *m/z*
(A)	$[Ru(PAID)(p\text{-cym})]^+$	560.092	560.091
(B)	$[Ru(PAID)(p\text{-cym})(H_2O)]^+$	578.102	578.102
(C) inset	$[Ru(PAIDH)(p\text{-}cym)Cl]^+$	596.069	596.068

Fig. S17 ESI-MS spectra of hydrolysis study of complex **1** incubated with 2:8 *v/v* methanol and 10 mM phosphate buffer (pH 7.4) with 4 mM NaCl, recorded after 0.5 h. Spectra represents experimental and simulated *m/z* values along with isotopic resolution of monocationic complexes- (A) **1** without halide, (B) aquated complex & (C) overall speciation with the molecular ion peak in the inset (red border). All the simulated spectra are represented in red colour. PAID = anionic form of the ligand PAIDH.

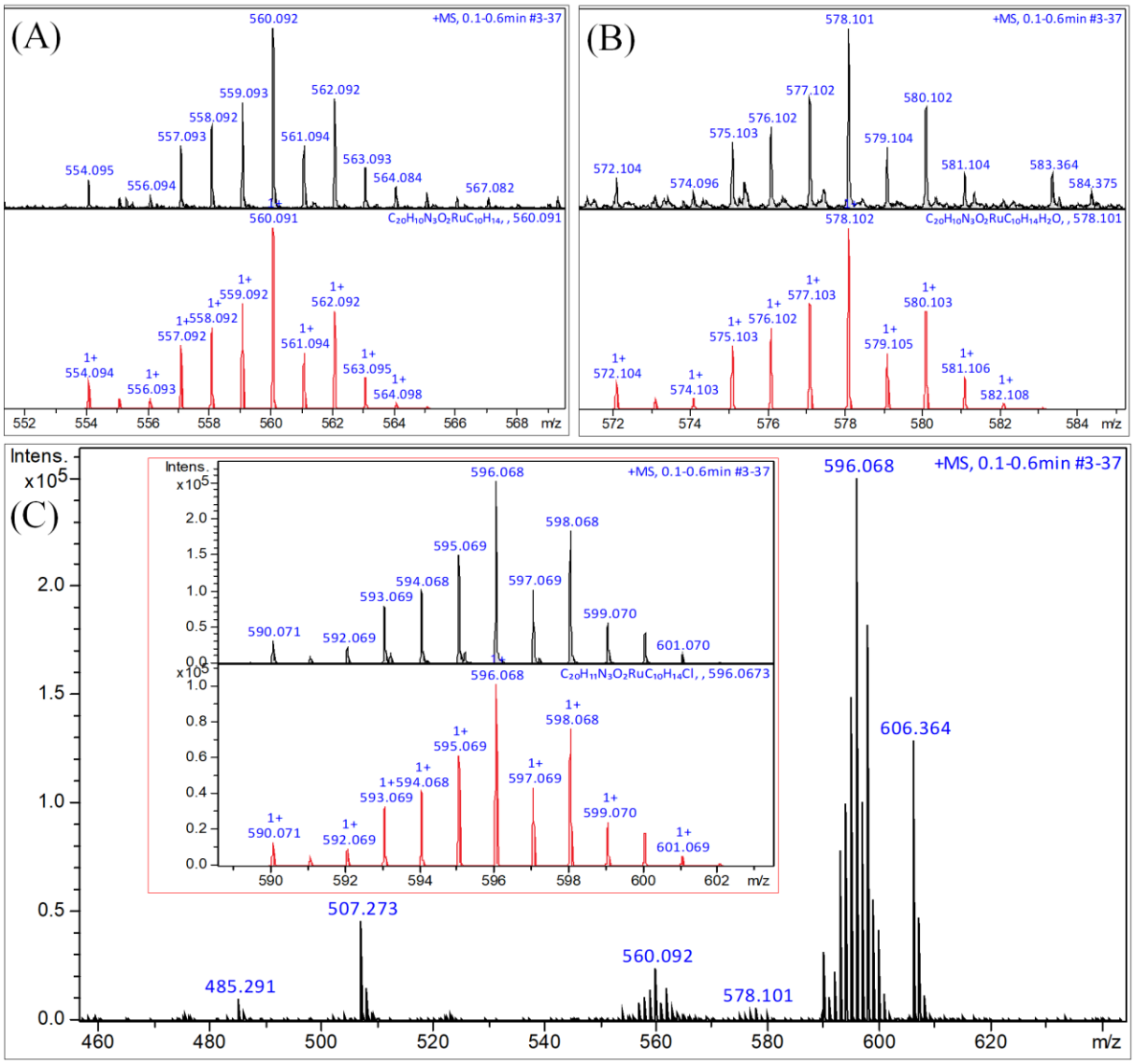

Figure	species	Exp. *m/z*	Calc. *m/z*
(A)	[Ru(PAID)(*p*-cym)]$^+$	560.092	560.091
(B)	[Ru(PAID)(*p*-cym)(H_2O)]$^+$	578.101	578.102
(C) inset	[Ru(PAIDH)(*p*-cym)Cl]$^+$	596.068	596.068

Fig. S18 ESI-MS spectra of hydrolysis study of complex **1** incubated with 2:8 *v/v* methanol and 10 mM phosphate buffer (pH 7.4) with 4 mM NaCl, recorded after 24 h. Spectra represents experimental and simulated *m/z* values along with isotopic resolution of monocationic complexes- (A) **1** without halide, (B) aquated complex & (C) overall speciation with the molecular ion peak in the inset (red border). All the simulated spectra are represented in red colour. PAID = anionic form of the ligand PAIDH.

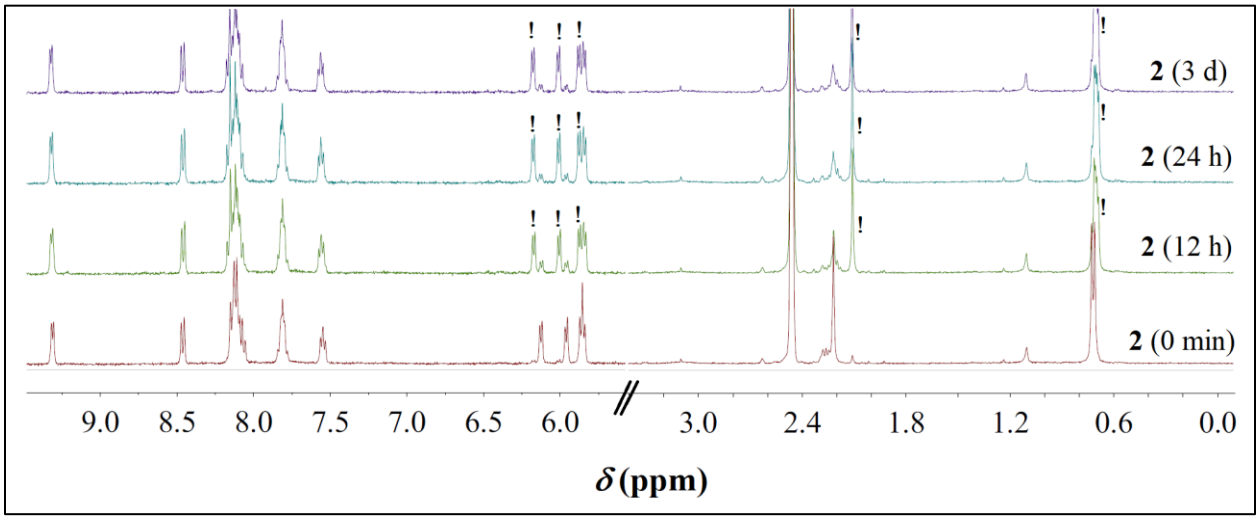

Fig. S19 ^{1}H NMR kinetic experiments to study hydrolysis of complex **2** in PBS buffer solution (pH = 7.4) in presence of 110 mM NaCl. '!' stands for the halide exchange forming **1** in solution. No arene loss is evident during the experiment for 3 days.

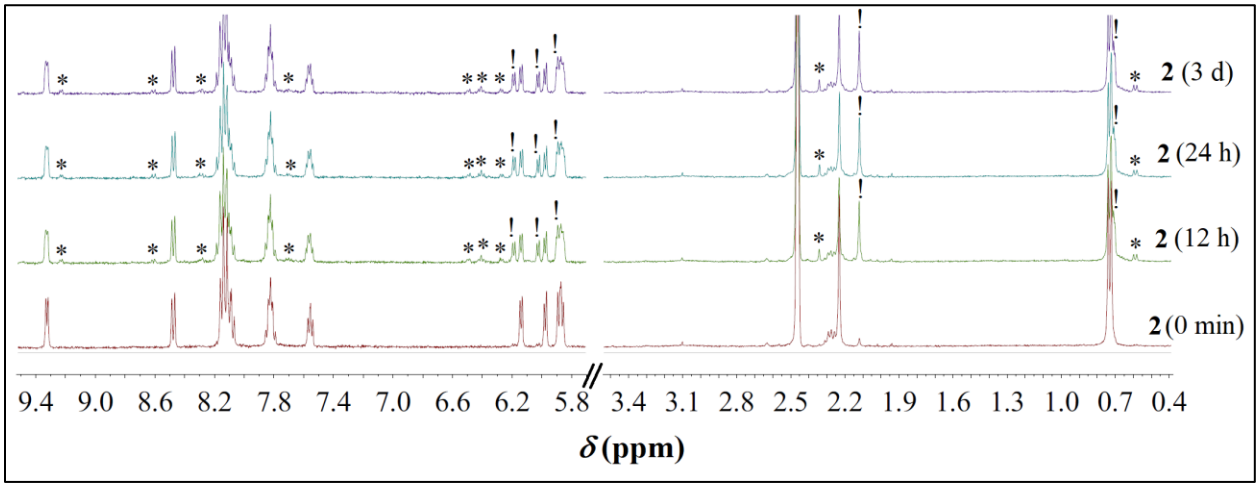

Fig. S20 ^{1}H NMR kinetic experiments to study hydrolysis of complex **2** in PBS buffer solution (pH = 7.4) in presence of 4 mM NaCl. '**!**' denotes the peaks arising due to halide exchange to form **1**. '*****' denotes the hydrolyzed peaks.

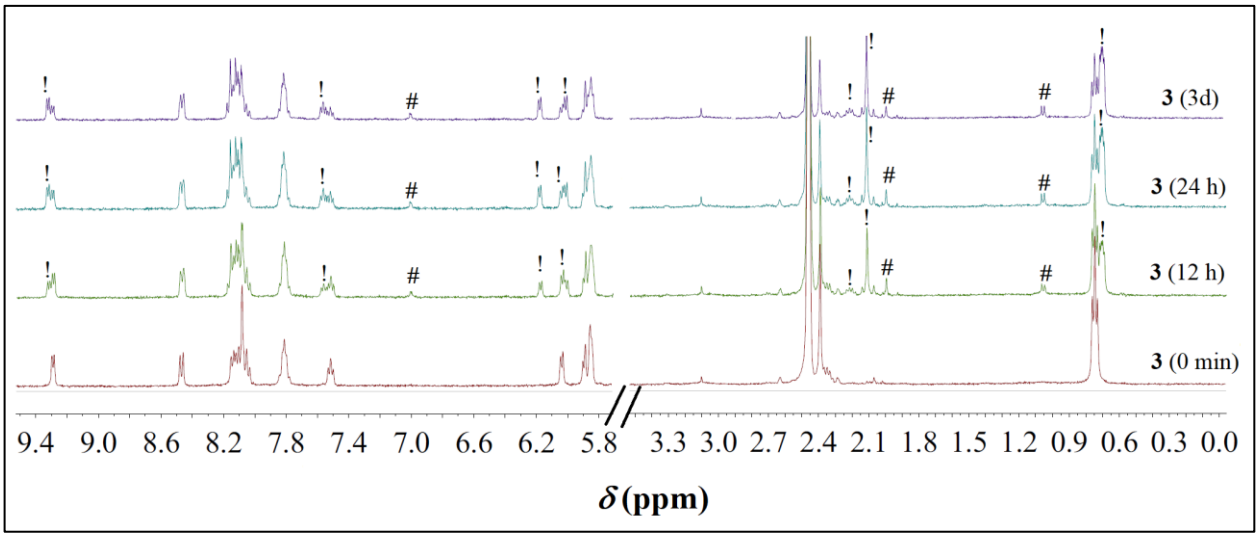

Fig. S21 ^{1}H NMR kinetic experiments to study hydrolysis of complex **3** in PBS buffer solution (pH = 7.4) in presence of 110 mM NaCl. '**!**' denotes the peaks arising due to halide exchange to form **1** and '**#**' stands for the peak of arene after loss from the metal center. No hydrolyzed peaks were observed during the course of the experiment for 3 days.

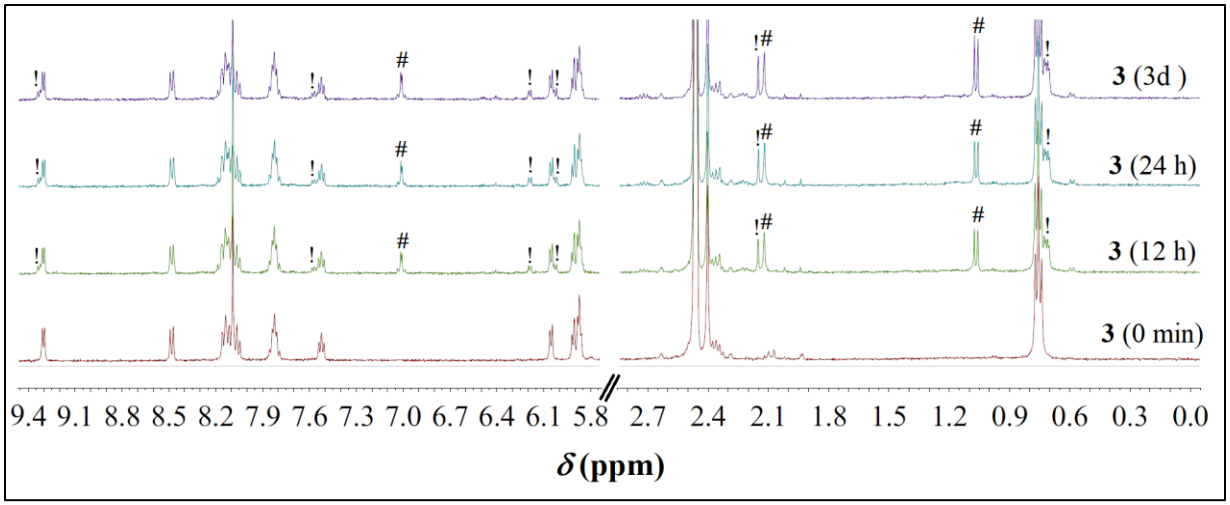

Fig. S22 ^{1}H NMR kinetic experiments to study hydrolysis of complex **3** in PBS buffer solution (pH = 7.4) in presence of 4 mM NaCl. '**!**' denotes the peaks arising due to halide exchange leading to formation of **1** and '**#**' stands for the peak of arene after loss from the metal center. No hydrolyzed peaks were observed during the course of the experiment for 3 days.

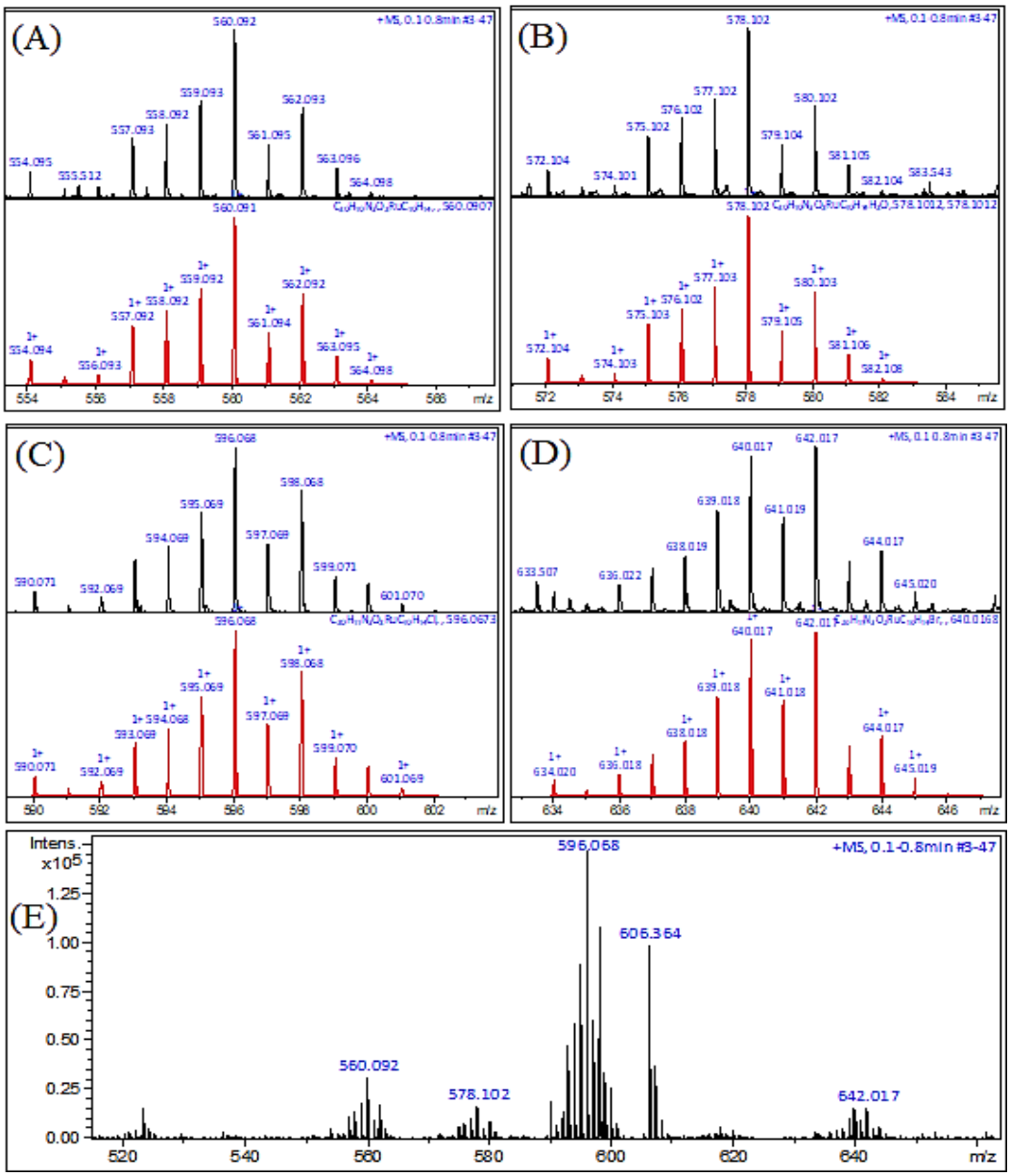

Figure	species	Exp. *m/z*	Calc. *m/z*
(A)	[Ru(PAID)(*p*-cym)]$^{+}$	560.092	560.091
(B)	[Ru(PAID)(*p*-cym)(H_2O)]$^{+}$	578.102	578.102
(C)	[Ru(PAIDH)(*p*-cym)Cl]$^{+}$	596.068	596.068
(D)	[Ru(PAIDH)(*p*-cym)Br]$^{+}$	640.017	640.017

Fig. S23 ESI-MS spectra of hydrolysis study of complex **2** incubated with 2:8 *v/v* methanol and 10 mM phosphate buffer (pH 7.4) with 4 mM NaCl, recorded after 0.5 h. Spectra represents experimental and simulated *m/z* values along with isotopic resolution of monocationic complexes- (A) complex without halide, (B) aquated complex, (C) Chloride exchange forming **1** from **2,** (D) molecular ion peak of **2** and (E) overall speciation. All the simulated spectra are represented in red colour. PAID = anionic form of the ligand PAIDH.

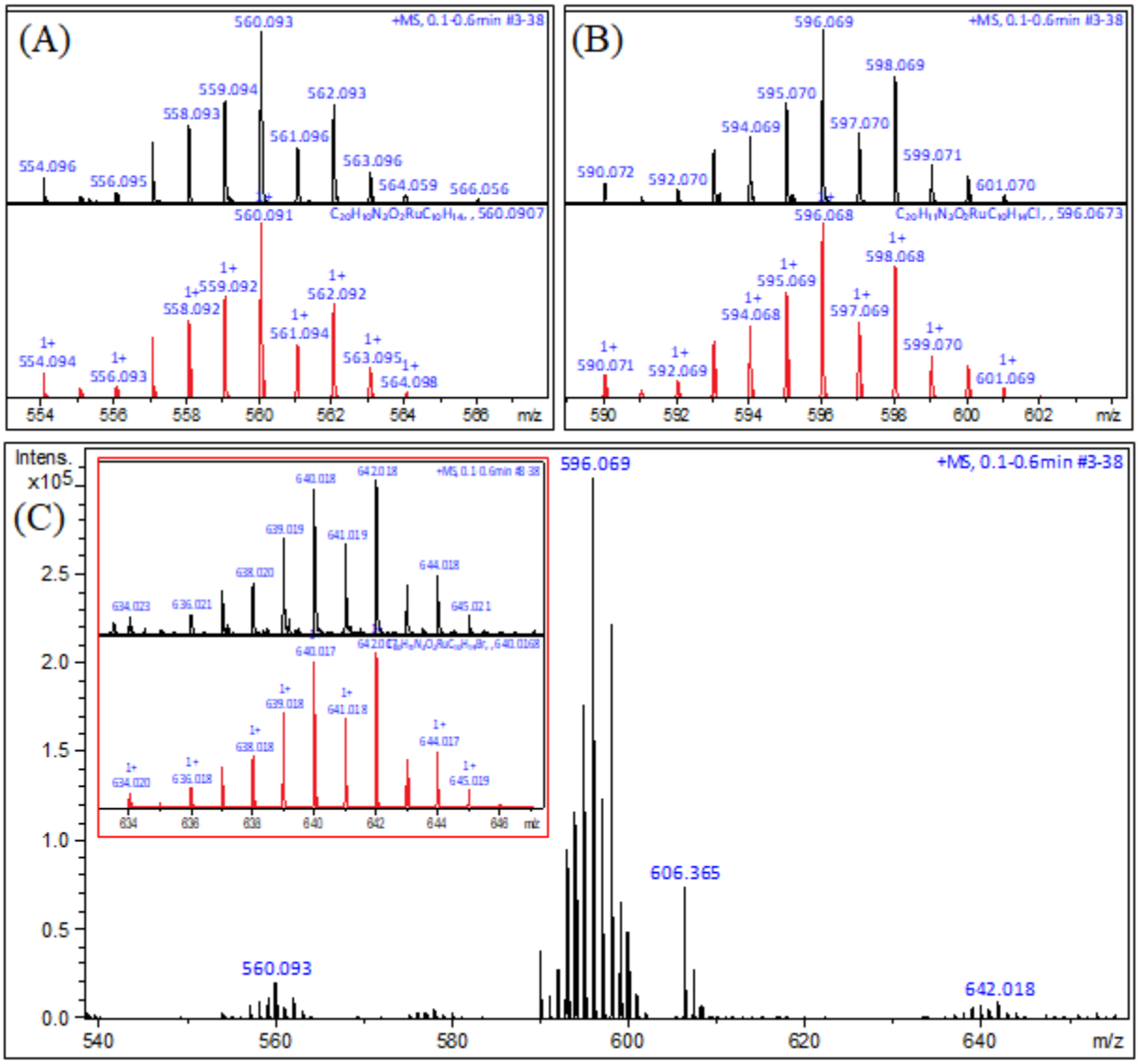

Figure	species	Exp. *m/z*	Calc. *m/z*
(A)	[Ru(PAID)(*p*-cym)]$^{+}$	560.093	560.091
(B)	[Ru(PAIDH)(*p*-cym)Cl]$^{+}$	596.069	596.068
(C)	[Ru(PAIDH)(*p*-cym)Br]$^{+}$	640.018	640.017

Fig. S24 ESI-MS spectra of hydrolysis study of complex **2** incubated with 2:8 *v/v* methanol and 10 mM phosphate buffer (pH 7.4) with 4 mM NaCl, recorded after 24 h. Spectra represents experimental and simulated *m/z* values along with isotopic resolution of monocationic complexes- (A) complex without halide, (B) Chloride exchange forming **1** from **2** and (C) overall speciation with the molecular ion peak in the inset (red border). All the simulated spectra are represented in red colour. PAID = anionic form of the ligand PAIDH.

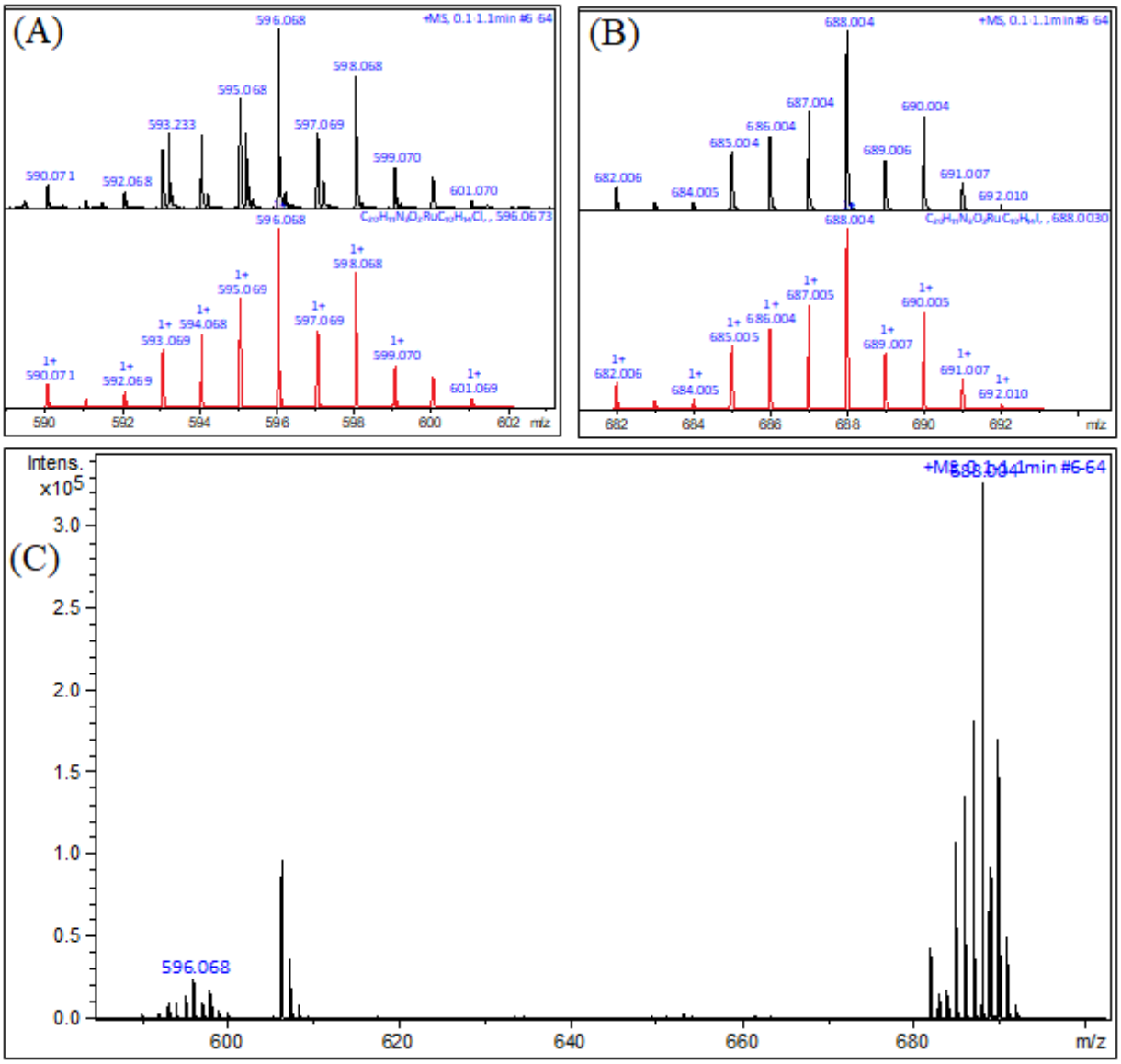

Figure	species	Exp. *m/z*	Calc. *m/z*
(A)	$[Ru(PAIDH)(p\text{-cym})Cl]^+$	596.068	596.068
(B)	$[Ru(PAIDH)(p\text{-cym})I]^+$	688.004	688.004

Fig. S25 ESI-MS spectra of hydrolysis study of complex **3** incubated with 2:8 *v/v* methanol and 10 mM phosphate buffer (pH 7.4) with 4 mM NaCl, recorded after 0.5 h. Spectra represents experimental and simulated *m/z* values along with isotopic resolution of monocationic complexes- (A) Chloride exchange forming **1** from **3** in very small amount, (B) molecular ion peak of **3** and (C) overall speciation. All the simulated spectra are represented in red colour.

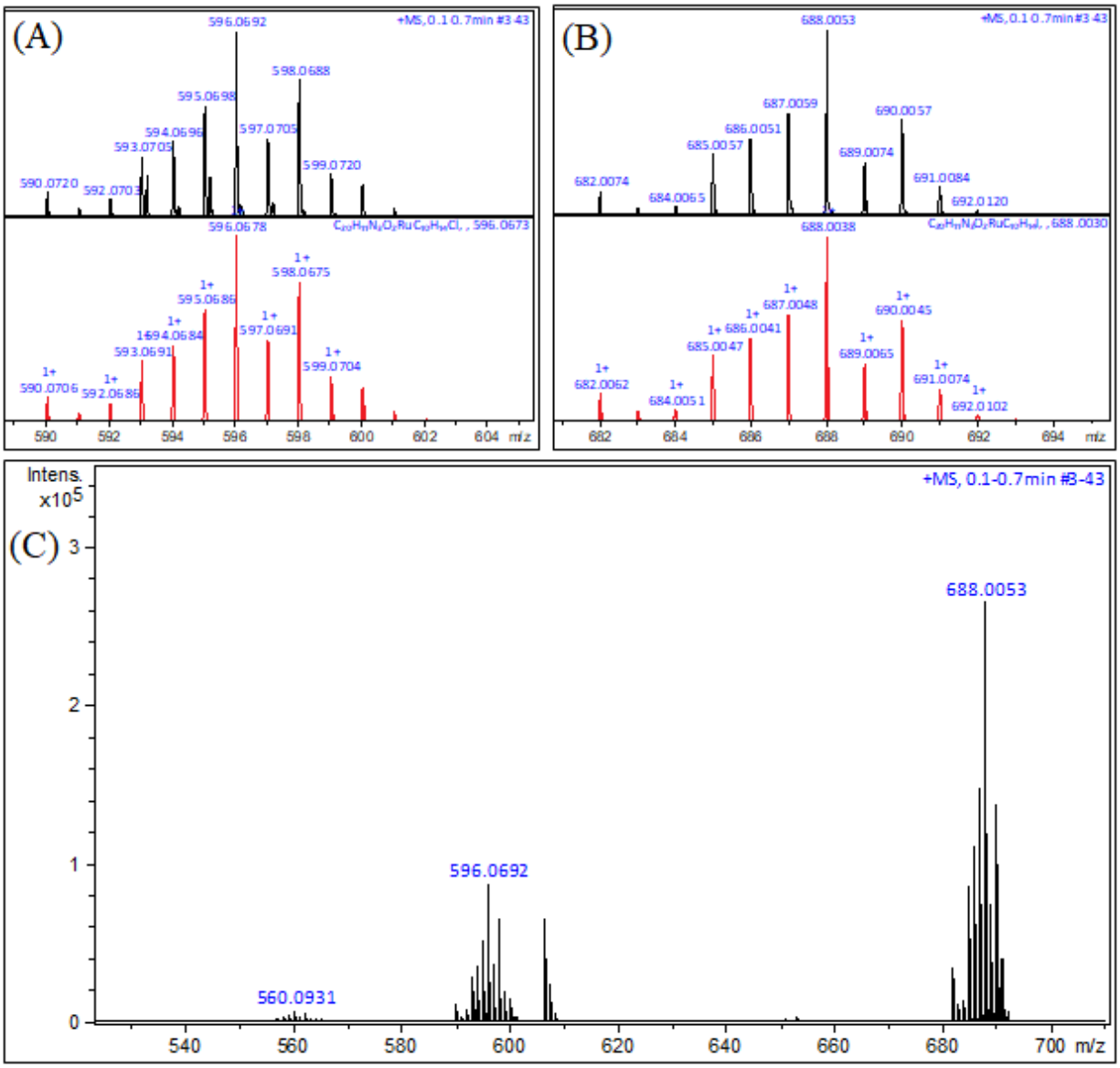

Figure	species	Exp. *m/z*	Calc. *m/z*
(A)	[Ru(PAIDH)(*p*-cym)Cl]$^+$	596.069	596.068
(B)	[Ru(PAIDH)(*p*-cym)I]$^+$	688.005	688.004
(C)	[Ru(PAID)(*p*-cym)]$^+$	560.093	560.091

Fig. S26 ESI-MS spectra of hydrolysis study of complex **3** incubated with 2:8 *v/v* methanol and 10 mM phosphate buffer (pH 7.4) with 4 mM NaCl, recorded after 24 h, shows exchange of halide is much less compared to **2**. Spectra represents experimental and simulated *m/z* values along with isotopic resolution of monocationic complexes- (A) Chloride exchange forming **1** from **3** in very small amount, (B) molecular ion peak of **3** and (C) overall speciation. All the simulated spectra are represented in red colour. PAID = anionic form of the ligand PAIDH.

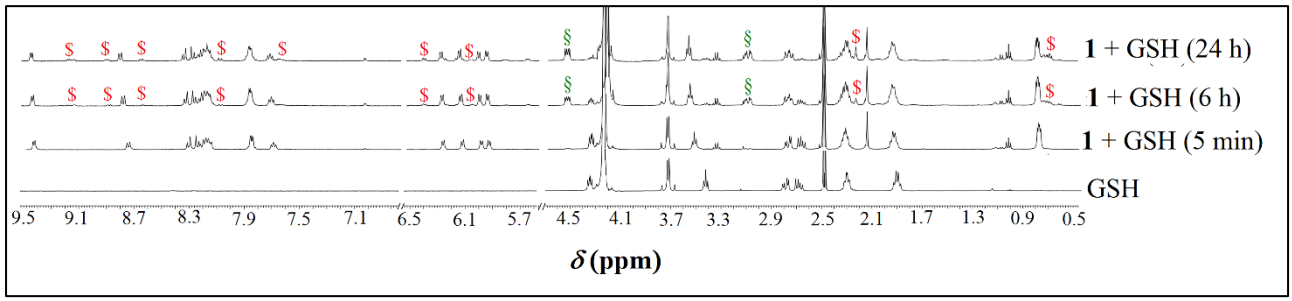

Fig. S27 Stack plot of ^{1}H NMR spectra of reduced L-glutathione (below), complex **1** and reduced L-glutathione (all the three from above) in DMSO-d_6/D_2O 7:3 (*v/v*) mixture, recorded at different interval of time at 25 °C. '**§**' stands for GSH auto-oxidation product, '**$**' GSH bound peaks.

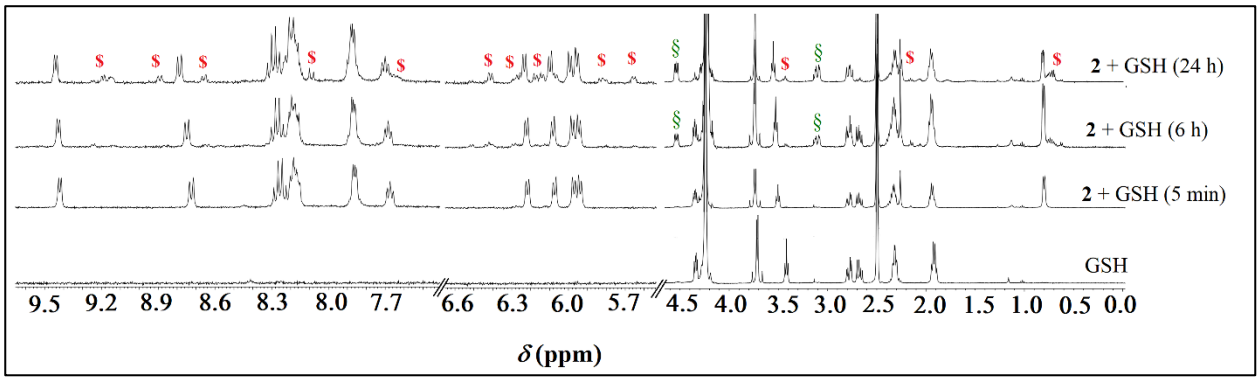

Fig. S28 Stack plot of ^{1}H NMR spectra of reduced L-glutathione (below), complex **2** and reduced L-glutathione (all the three from above) in DMSO-d_6/D_2O 7:3 (*v/v*) mixture, recorded at different interval of time at 25°C. '**§**' stands for GSH auto-oxidation product, '**$**' GSH bound peaks corresponding to both $[(PAIDH)Ru^{II}(p\text{-cym})(GS)]^{+}$ and $[Ru^{II}(p\text{-cym})(GS)]^{+}$.

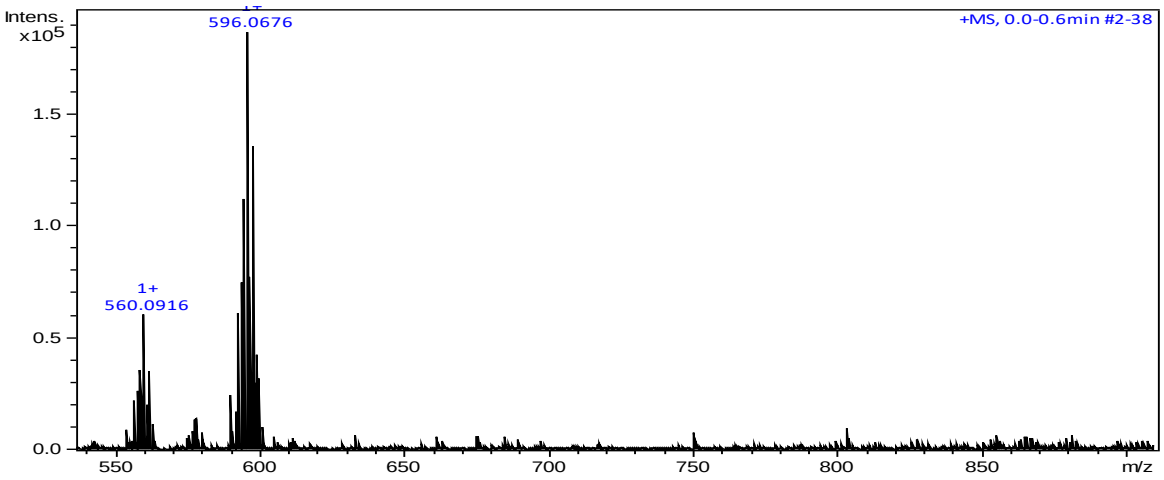

species	Exp. *m/z*	Calc. *m/z*
$[Ru(PAID)(p\text{-cym})]^+$	560.092	560.091
$[Ru(PAID)(p\text{-cym})(H_2O)]^+$	578.101	578.102
$[Ru(PAIDH)(p\text{-cym})Cl]^+$	596.068	596.068

Fig. S29 ESI-MS spectrum of glutathione (GSH) interaction with complex **1** using 1:2.5 mol ratio of complex:GSH. Incubation in 2:8 *v/v* methanol and 4 mM aqueous NaCl, recorded after 2 h. No GSH adduct with **1** was found.

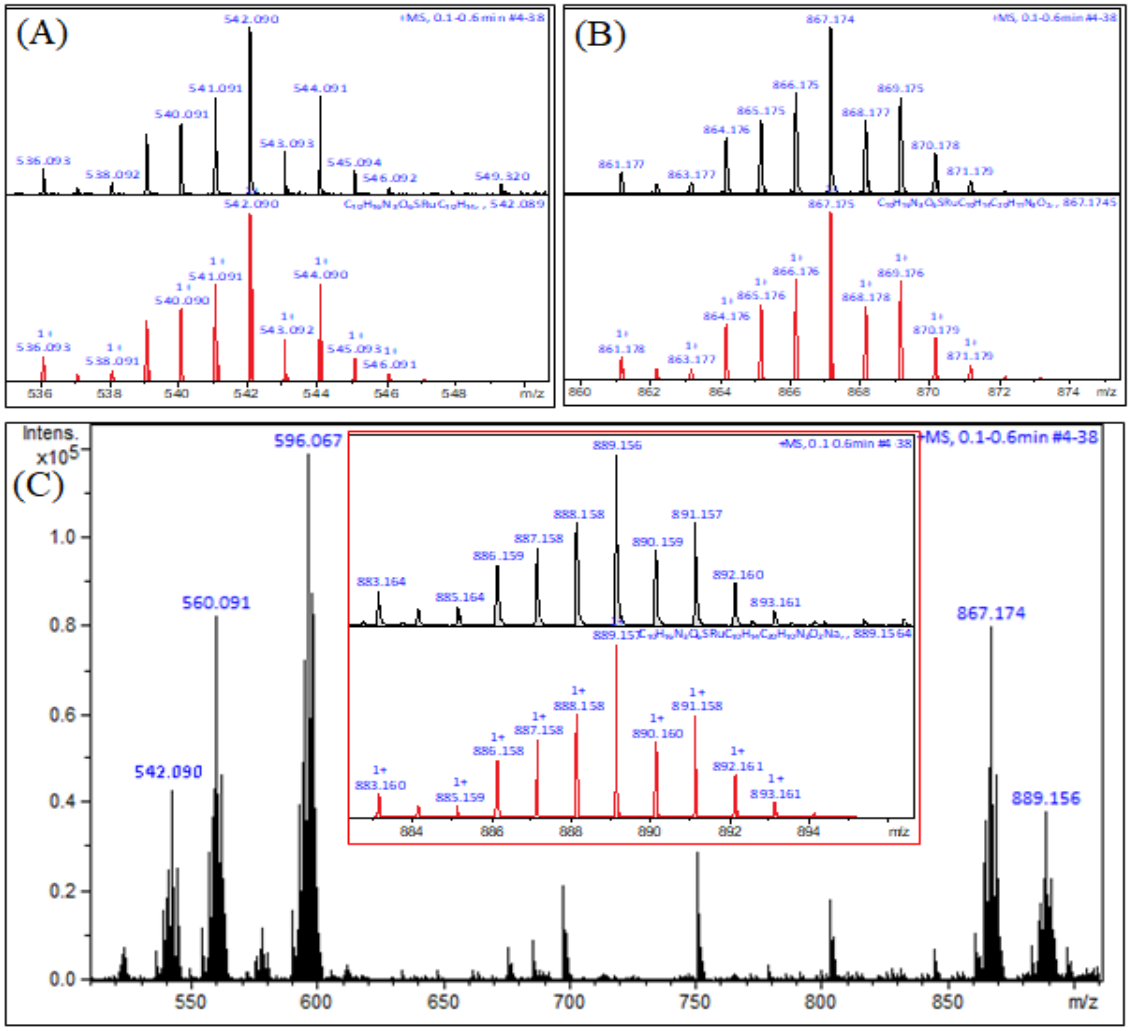

species	Exp. *m/z*	Calc. *m/z*
$[Ru(GS)(p\text{-cym})]^+$	542.090	542.089
$[Ru(PAID)(p\text{-cym})]^+$	560.091	560.091
$[Ru(PAID)(p\text{-cym})(H_2O)]^+$	578.101	578.102
$[Ru(PAIDH)(p\text{-cym})Cl]^+$	596.067	596.068
$[Ru(PAIDH)(GS)(p\text{-cym})]^+$	867.174	867.175
$[Ru(PAID)(GS)(p\text{-cym})]Na^+$	889.156	889.157

Fig. S30 ESI-MS spectrum of GSH interaction with complex **1** using 1:2.5 mole ratio of complex:GSH. Incubation in 2:8 *v/v* methanol and 4 mM aqueous NaCl, recorded after 24 h. The overall peak intensities show that there has been increase in GSH adduct intensity. Spectra represents experimental and simulated *m/z* values along with isotopic resolution of monocationic complexes- (A) PAIDH dissociated GSH bound metal complex, $[Ru(GS)(p\text{-cym})]^+$, (B) GSH adduct of halide dissociated complex, $[Ru(PAIDH)(GS)(p\text{-cym})]^+$ and (C) overall speciation (inset: sodiated GSH adduct of **1**, $[Ru(PAID)(GS)(p\text{-cym})]Na^+$). All the simulated spectra are represented in red colour. [PAID = anionic form of the ligand PAIDH and GS = anionic glutathione]

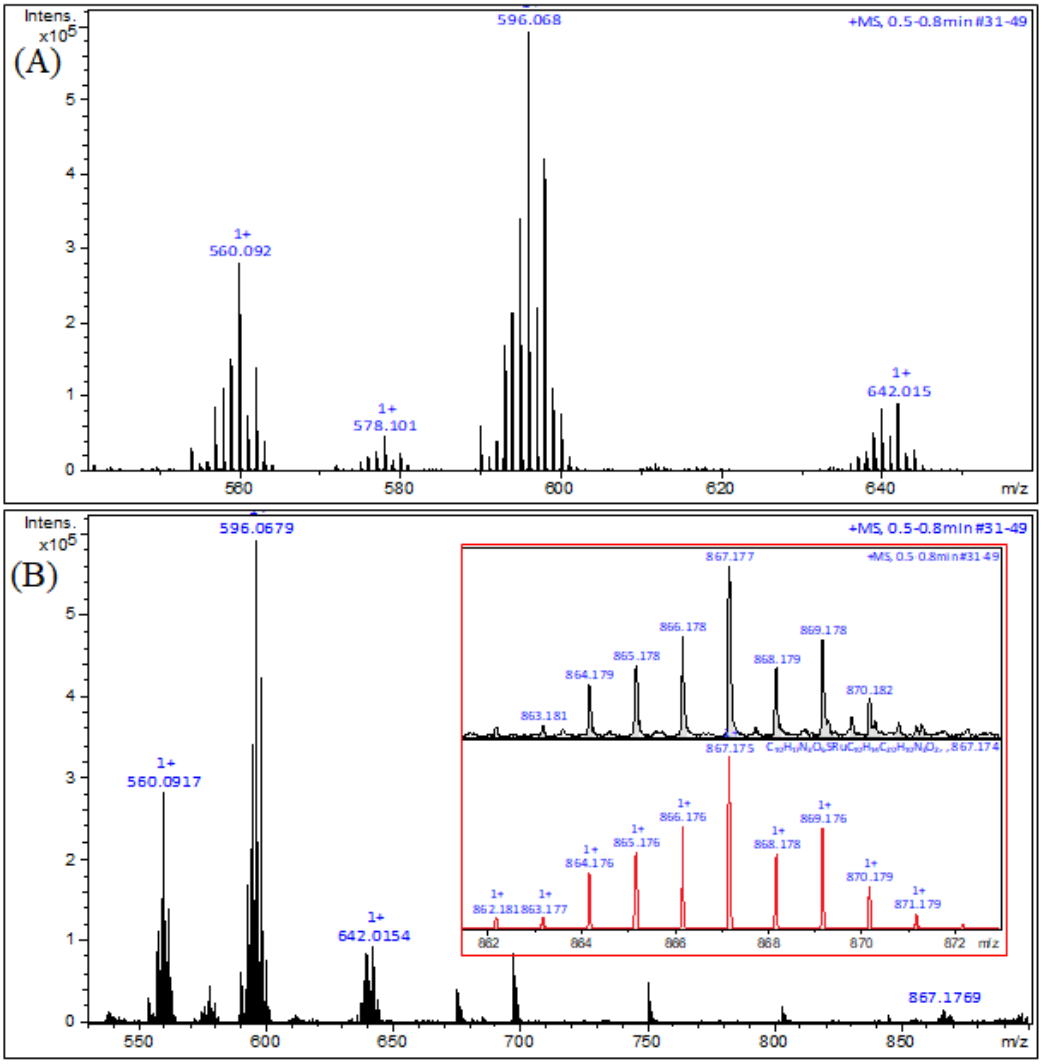

species	Exp. *m/z*	Calc. *m/z*
[Ru(PAID)(*p*-cym)]$^+$	560.092	560.091
[Ru(PAID)(*p*-cym)(H_2O)]$^+$	578.101	578.102
[Ru(PAIDH)(*p*-cym)Cl]$^+$	596.068	596.068
[Ru(PAIDH)(*p*-cym)Br]$^+$	640.015	640.017
[Ru(PAIDH)(*p*-cym)(GS)]$^+$	867.177	867.175

Fig. S31 ESI-MS spectrum of GSH interaction with complex **2** using 1:2.5 mole ratio of complex:GSH. Incubation in 2:8 *v/v* methanol and 4 mM aqueous NaCl, recorded after 2 h. The overall peak intensities show that there is more GSH adduct than that of **1**. Spectra shows isotopic resolution of monocationic complexes- (A) magnified view showing the halide dissociated **2**, aquated species, chloride exchange forming **1** from **2**, molecular ion peak of **2** and (B) over all speciation (inset: GSH adduct of **2**, [Ru(PAIDH)(GS)(*p*-cym)]$^+$). All the simulated spectra are represented in red colour. [PAID = anionic form of the ligand PAIDH and GS = anionic glutathione]

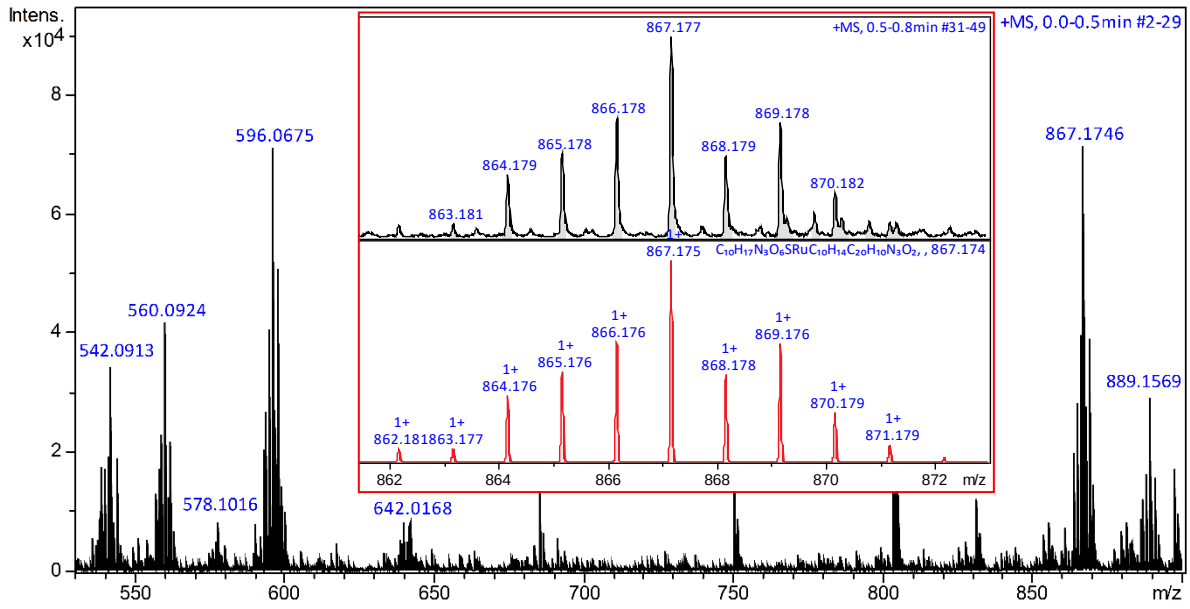

species	Exp. *m/z*	Calc. *m/z*
[Ru(*p*-cym)(GS)]$^+$	542.091	542.089
[Ru(PAID)(*p*-cym)]$^+$	560.092	560.091
[Ru(PAID)(*p*-cym)(H_2O)]$^+$	578.102	578.102
[Ru(PAIDH)(*p*-cym)Cl]$^+$	596.067	596.068
[Ru(PAIDH)(*p*-cym)Br]$^+$	640.017	640.017
[Ru(PAIDH)(*p*-cym)(GS)]$^+$	867.175	867.175
[Ru(PAID)(*p*-cym)(GS)]Na$^+$	889.157	889.157

Fig. S32 ESI-MS spectrum of GSH interaction with complex **2** using 1:2.5 mol ratio of complex:GSH. Incubation in 2:8 *v/v* methanol and 4 mM aqueous NaCl, recorded after 24 h. The overall peak intensities show that the most intense is the GSH adduct peak. Spectra shows isotopic resolution of monocationic complexes showing PAIDH dissociated GSH bound metal complex, [Ru(*p*-cym)(GS)]$^+$; the halide dissociated **2**, [Ru(PAID)(*p*-cym)]$^+$; aquated species, [Ru(PAID)(*p*-cym)(H_2O)]$^+$; chloride exchange forming **1** from **2**, [Ru(PAIDH)(*p*-cym)Cl]$^+$; molecular ion peak of **2**, [Ru(PAIDH)(*p*-cym)Br]$^+$; GSH adduct of **2**, [Ru(PAIDH)(GS)(*p*-cym)]$^+$) and [Ru(PAID)(*p*-cym)(GS)]Na$^+$. [PAID = anionic form of the ligand PAIDH and GS = anionic glutathione]

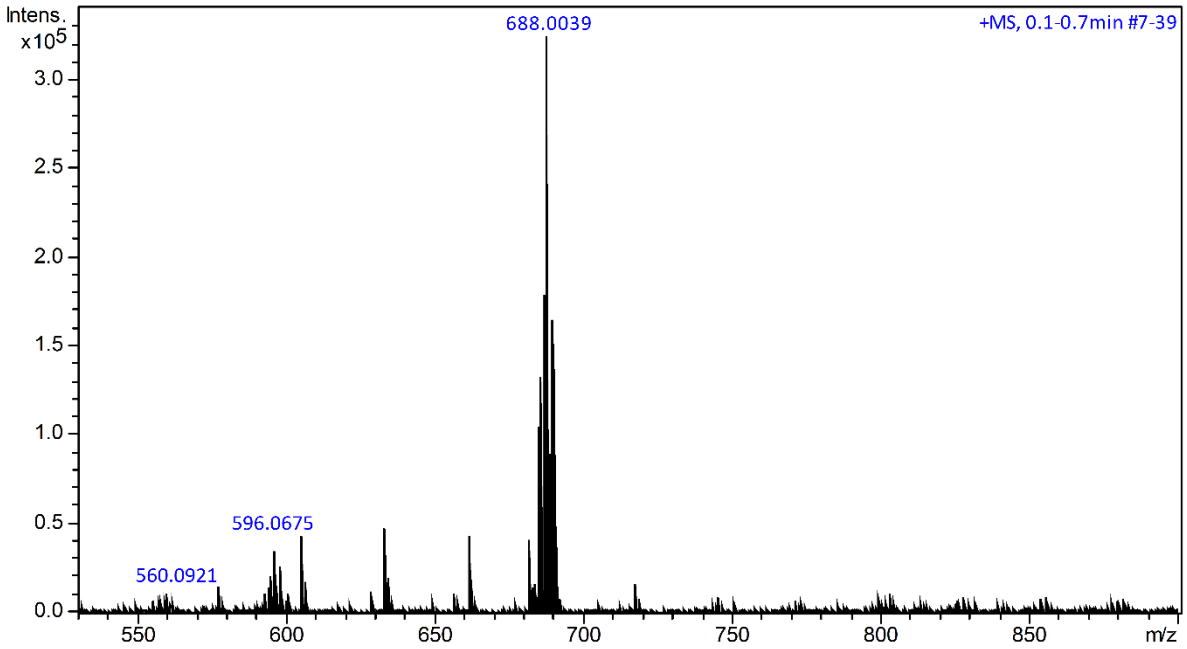

species	Exp. *m/z*	Calc. *m/z*
[Ru(PAID)(*p*-cym)]$^+$	560.092	560.091
[Ru(PAIDH)(*p*-cym)Cl]$^+$	596.068	596.068
[Ru(PAIDH)(*p*-cym)I]$^+$	688.004	688.004

Fig. S33 ESI-MS spectrum of GSH interaction with complex **3** using 1:2.5 mol ratio of complex:GSH. Incubation in 2:8 *v/v* methanol and 4 mM aqueous NaCl, recorded after 2 h. The overall peak intensities show that there is no adduct formation with GSH, unlike complex **2**.

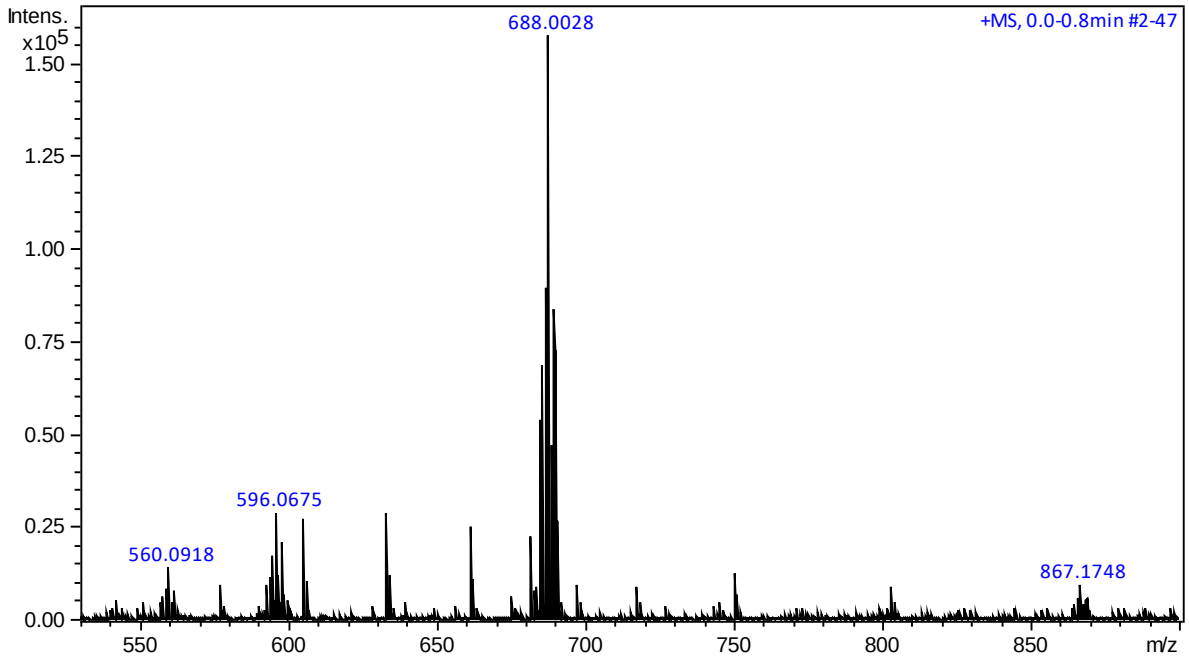

species	Exp. *m/z*	Calc. *m/z*
[Ru(PAID)(*p*-cym)]$^+$	560.092	560.091
[Ru(PAIDH)(*p*-cym)Cl]$^+$	596.068	596.068
[Ru(PAIDH)(*p*-cym)I]$^+$	688.003	688.004
[Ru(PAIDH)(*p*-cym)(GS)]$^+$	867.175	867.175

Fig. S34 ESI-MS spectrum of GSH interaction with complex **3** using 1:2.5 mol ratio of complex:GSH. Incubation in 2:8 *v/v* methanol and 4 mM aqueous NaCl, recorded after 24 h. The overall peak intensities show that there is very small amount of adduct formation with GSH even after 24 h, unlike complex **1** and **2**.

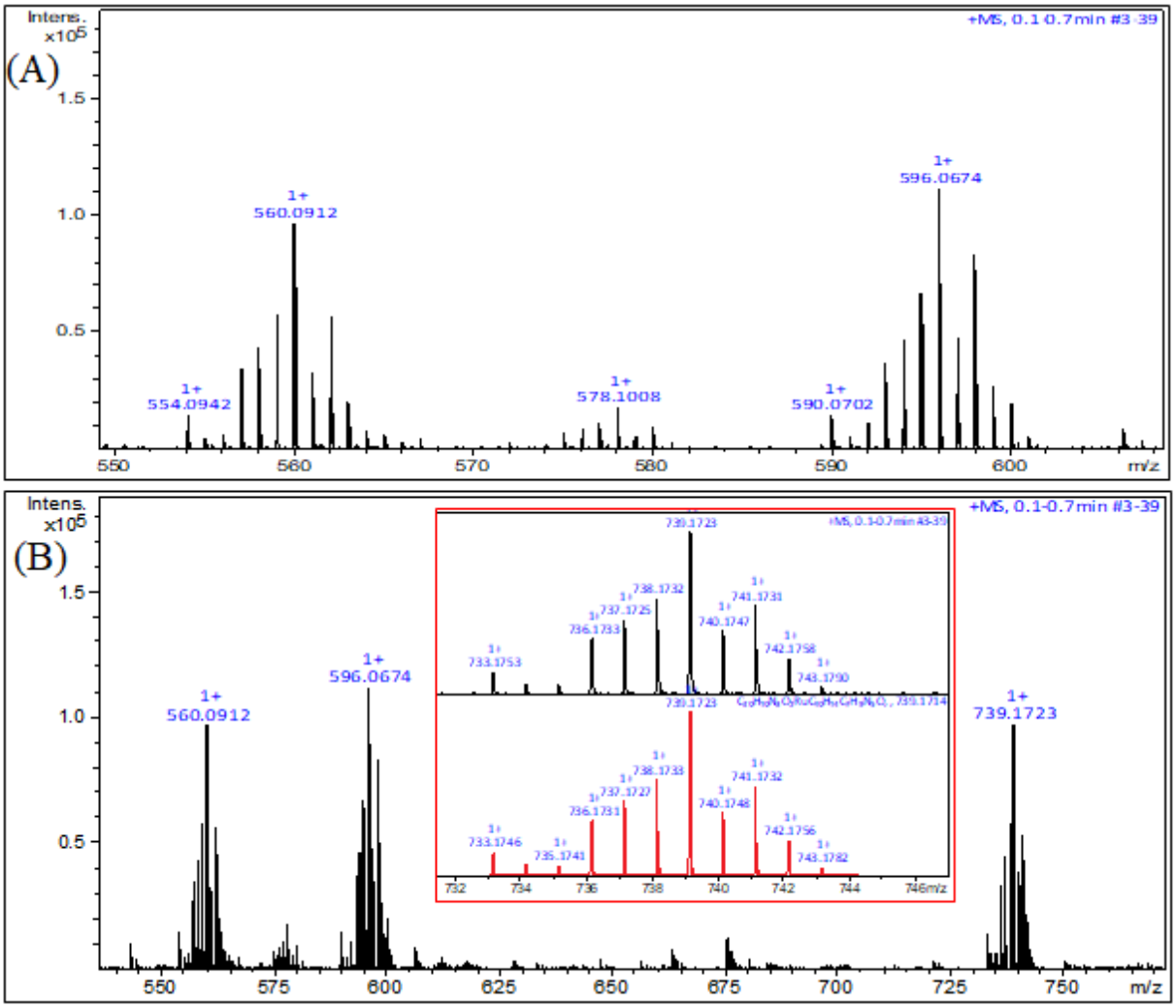

species	Exp. *m/z*	Calc. *m/z*
[Ru(PAID)(*p*-cym)]$^+$	560.091	560.091
[Ru(PAID)(*p*-cym)(H_2O)]$^+$	578.101	578.102
[Ru(PAIDH)(*p*-cym)Cl]$^+$	596.067	596.068
[Ru(PAIDH)(*p*-cym)(9-EtG)]$^+$	739.172	739.172

Fig. S35 ESI-MS spectra of 9-ethylguanine(9-EtG) interaction with complex **1** using 1:1 mol ratio of complex:9-EtG. Incubation in 2:8 *v/v* methanol and 4 mM aqueous NaCl, recorded after 2 h, showing 9-EtG bound complex. Spectra represents *m/z* values along with isotopic resolution of monocationic complexes- (A) magnified view showing the halide dissociated **1**, aquated species, molecular ion peak and (B) overall speciation with the 9-EtG bound **1** (inset: magnified view of the 9-EtG bound species along with the simulation). All the simulated spectra are represented in red colour. PAID = anionic form of the ligand PAIDH.

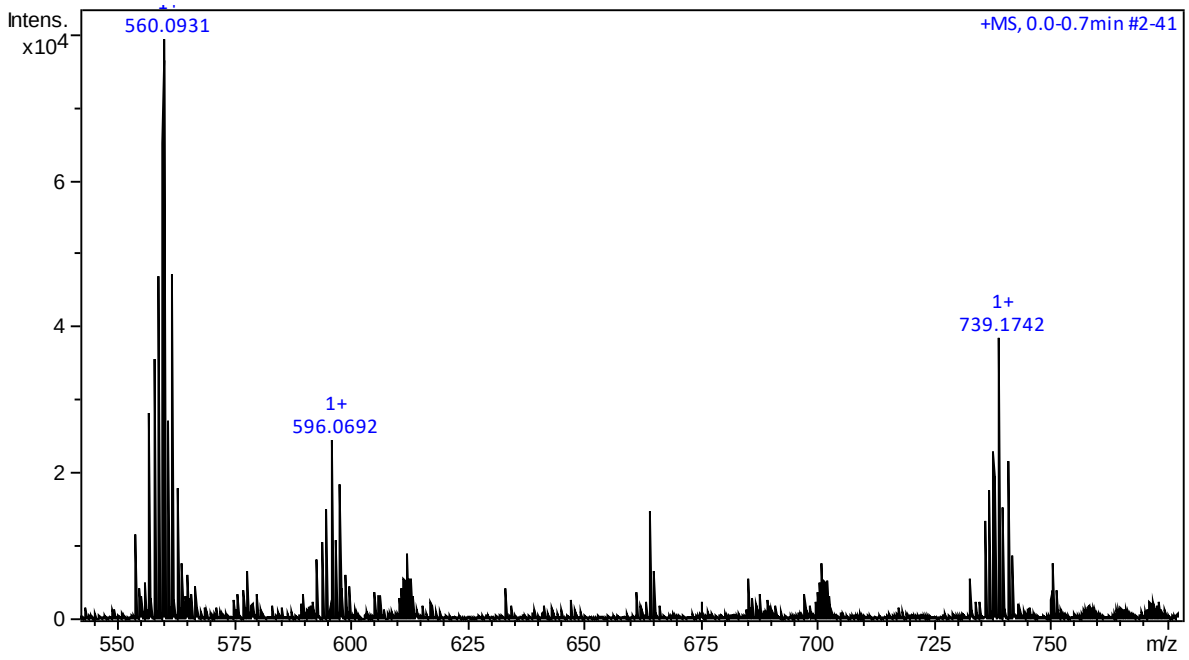

species	Exp. *m/z*	Calc. *m/z*
[Ru(PAID)(*p*-cym)]$^+$	560.093	560.091
[Ru(PAID)(*p*-cym)(H_2O)]$^+$	578.101	578.102
[Ru(PAIDH)(*p*-cym)Cl]$^+$	596.069	596.068
[Ru(PAIDH)(*p*-cym)(9-EtG)]$^+$	739.174	739.172

Fig. S36 ESI-MS spectrum of 9-ethylguanine(9-EtG) interaction with complex **1** using 1:1 mol ratio of complex:9-EtG. Incubation in 2:8 *v/v* methanol and 4 mM aqueous NaCl, recorded after 24 h, showing 9-EtG bound complex. The dehalogenated species concentration shows a ratio metric increase over a 24 h period.

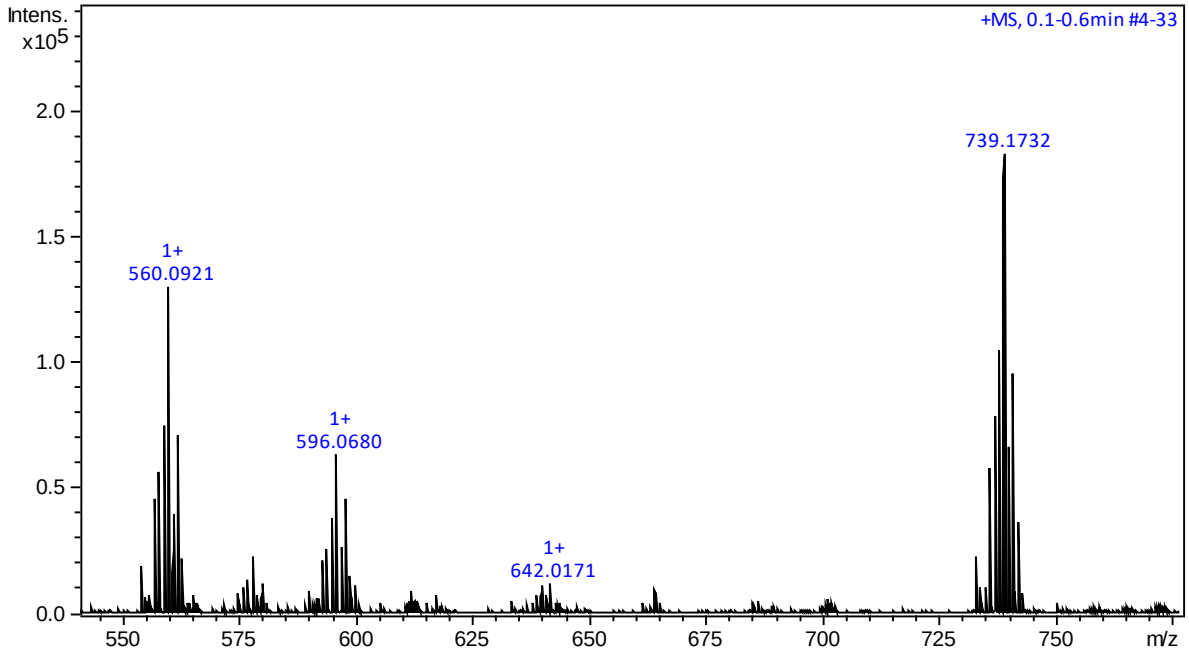

species	Exp. *m/z*	Calc. *m/z*
[Ru(PAID)(*p*-cym)]$^+$	560.092	560.091
[Ru(PAID)(*p*-cym)(H_2O)]$^+$	578.101	578.102
[Ru(PAIDH)(*p*-cym)Cl]$^+$	596.068	596.068
[Ru(PAIDH)(*p*-cym)Br]$^+$	640.017	640.017
[Ru(PAIDH)(*p*-cym)(9-EtG)]$^+$	739.173	739.172

Fig. S37 ESI-MS spectrum of 9-ethylguanine (9-EtG) interaction with complex **2** using 1:1 mol ratio of complex:9-EtG. Incubation in 2:8 *v/v* methanol and 4 mM aqueous NaCl, recorded after 2 h, showing that the most intense *m/z* corresponds to 9-EtG adduct with **2**.

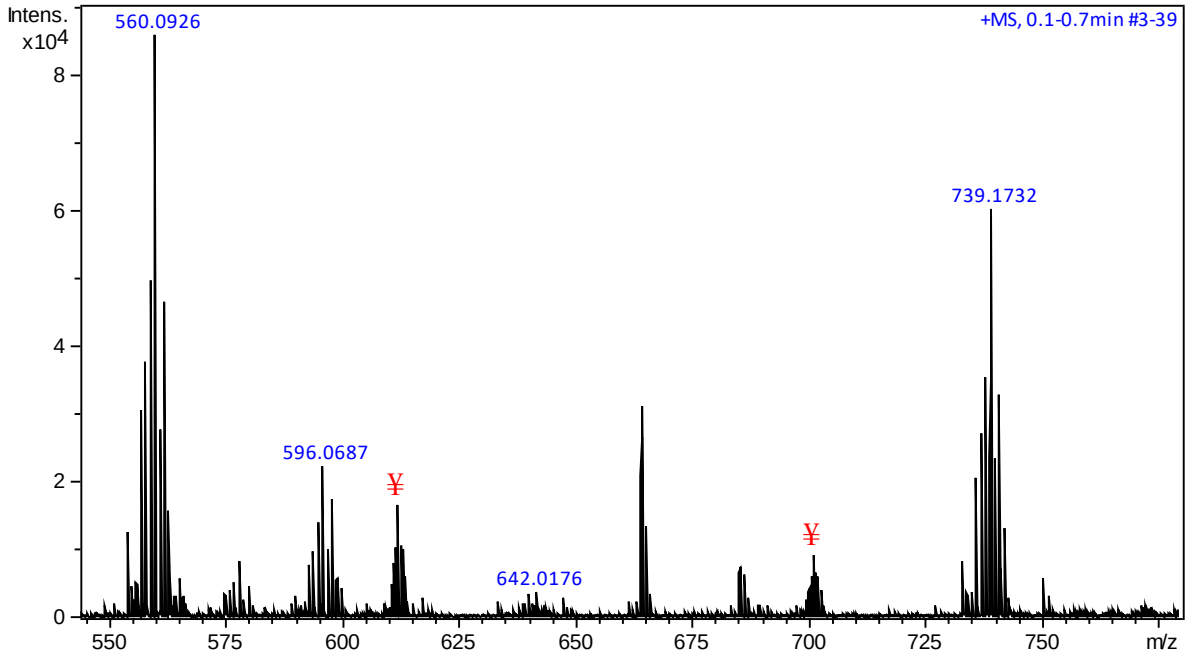

species	Exp. *m/z*	Calc. *m/z*
[Ru(PAID)(*p*-cym)]$^+$	560.093	560.091
[Ru(PAID)(*p*-cym)(H_2O)]$^+$	578.101	578.102
[Ru(PAIDH)(*p*-cym)Cl]$^+$	596.069	596.068
[Ru(PAIDH)(*p*-cym)Br]$^+$	640.018	640.017
[Ru(PAIDH)(*p*-cym)(9-EtG)]$^+$	739.173	739.172

Fig. S38 ESI-MS spectrum of 9-ethylguanine (9-EtG) interaction with complex **2** using 1:1 mol ratio of complex:9-EtG. Incubation in 2:8 *v/v* methanol and 4 mM aqueous NaCl, recorded after 24 h. The overall peak intensities show a decrease suggesting there may be degradation or precipitation of the complex from solution. '¥' stands for uncharacterized polynuclear Ru species.

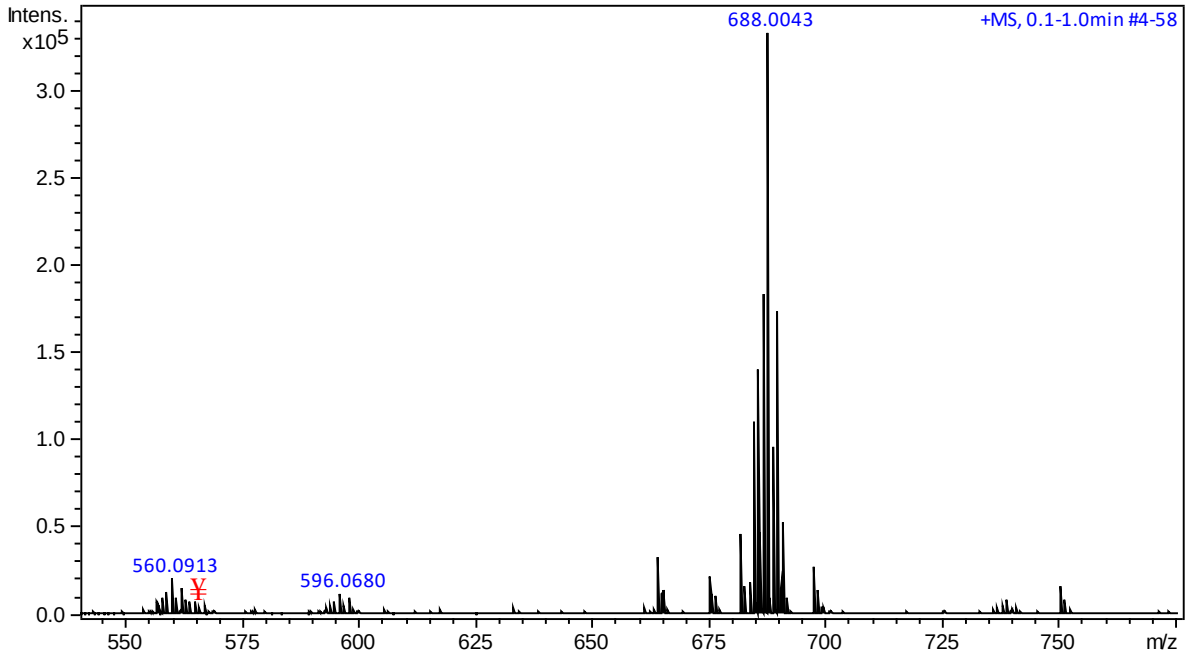

species	Exp. *m/z*	Calc. *m/z*
[Ru(PAID)(*p*-cym)]$^+$	560.091	560.091
[Ru(PAIDH)(*p*-cym)Cl]$^+$	596.068	596.068
[Ru(PAIDH)(*p*-cym)I]$^+$	688.004	688.004

Fig. S39 ESI-MS spectrum of 9-ethylguanine (9-EtG) interaction with complex **3** using 1:1 mol ratio of complex:9-EtG. Incubation in 2:8 *v/v* methanol and 4 mM aqueous NaCl, recorded after 2 h. The overall peak intensities show that there is hardly any adduct formation with 9-EtG. There is some '**¥**' uncharacterized polynuclear Ru species in the same place where the dehalogenated species appears.

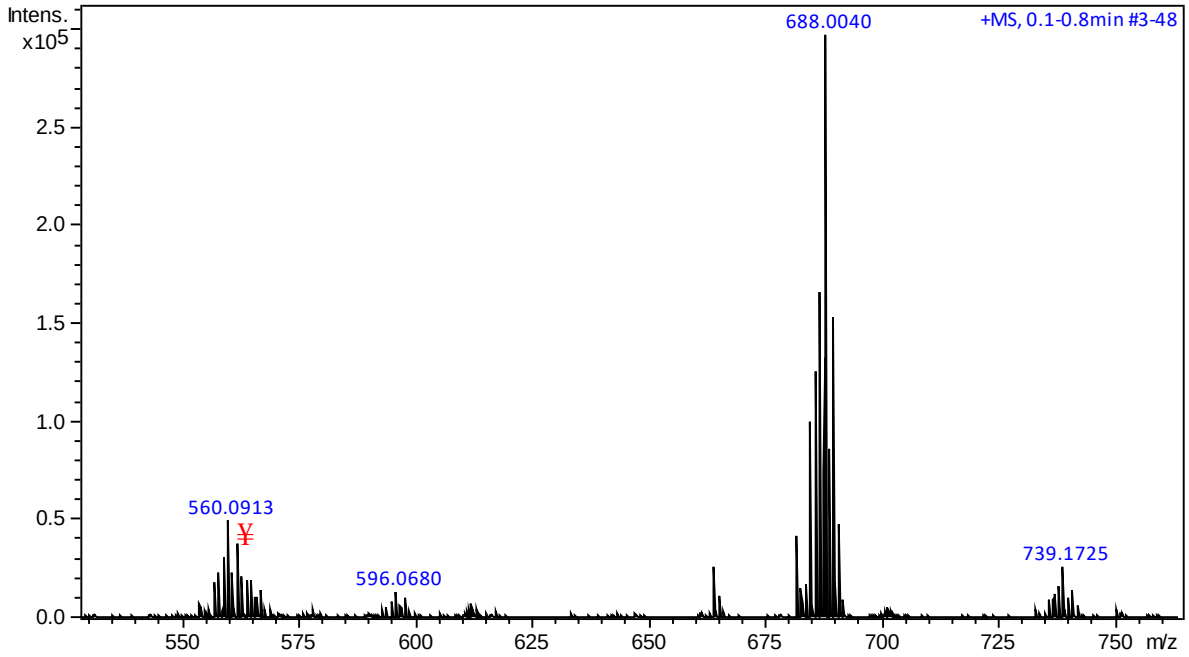

species	Exp. *m/z*	Calc. *m/z*
[Ru(PAID)(*p*-cym)]$^+$	560.091	560.091
[Ru(PAIDH)(*p*-cym)Cl]$^+$	596.068	596.068
[Ru(PAIDH)(*p*-cym)I]$^+$	688.004	688.004
[Ru(PAIDH)(*p*-cym)(9-EtG)]$^+$	739.173	739.172

Fig. S40 ESI-MS spectrum of 9-ethylguanine (9-EtG) interaction with complex **3** using 1:1 mol ratio of complex:9-EtG. Incubation in 2:8 *v/v* methanol and 4 mM aqueous NaCl, recorded after 24 h. The overall peak intensities show that there is formation of a small amount of adduct with 9-EtG. There is also some '¥' uncharacterized polynuclear Ru species in the same place where the dehalogenated species appears.

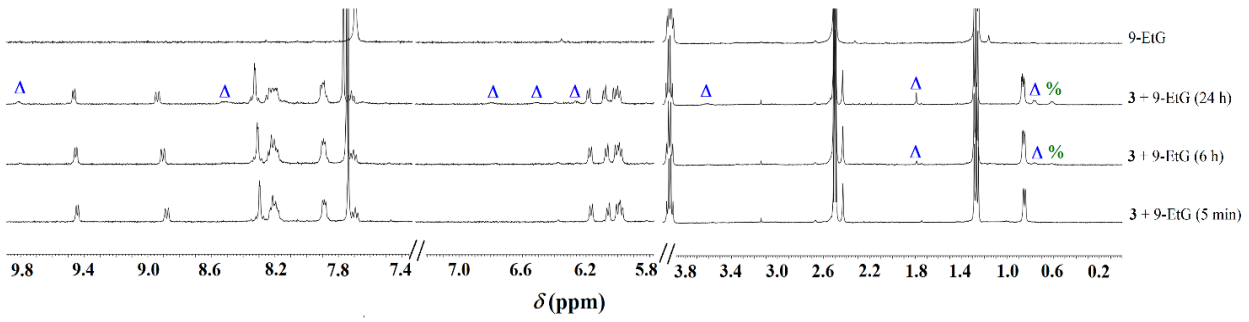

Fig. S41 9-Ethyl Guanine binding of **3** in DMSO-d_6/D_2O 7:3 (*v/v*) mixture, recorded at different interval of time at 25 °C. Recording started after 5 minutes of dissolving 9-Ethyl guanine and complex **3** together. '**Δ**' stands for the metal complex peaks and '**%**' stands for the 9-Ethyl guanine peaks of the 9-EtG bound metal complex species.

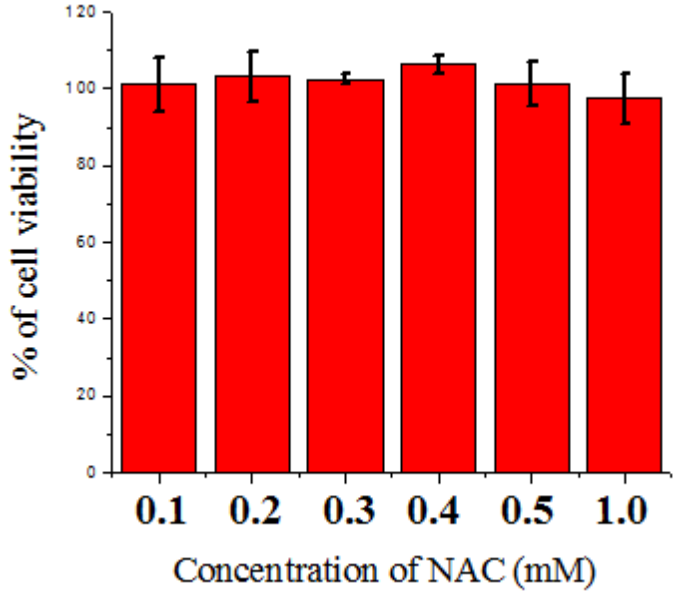

Fig. S42 Cytotoxicity of HepG2 cells under normoxic condition in presence of different concentration of N-acetyl cysteine (NAC). Concentration taken from 100 µM to 1 mM.

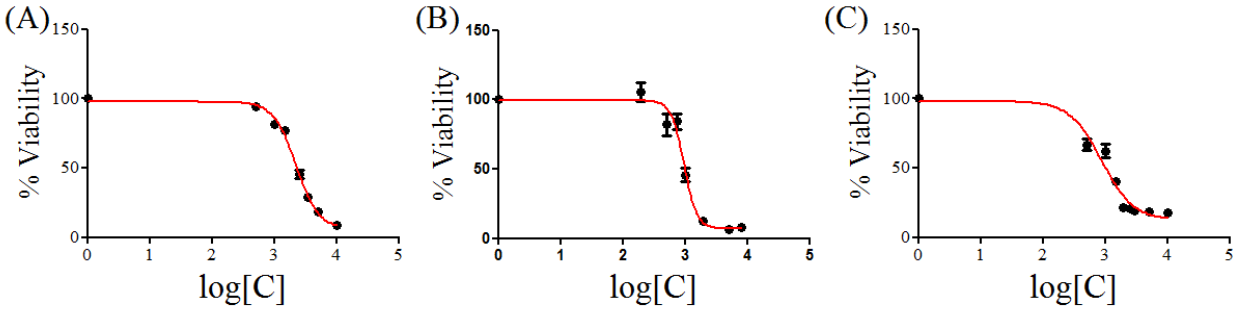

Fig. S43 Plots of cell viability (%) vs. log of concentrations of **1**-**3** against HepG2 cell line after incubation for 48 h determined from MTT assays under normoxic condition. The plots provided are for one independent experiment (each concentration in triplicate) out of at least three independent experiments.

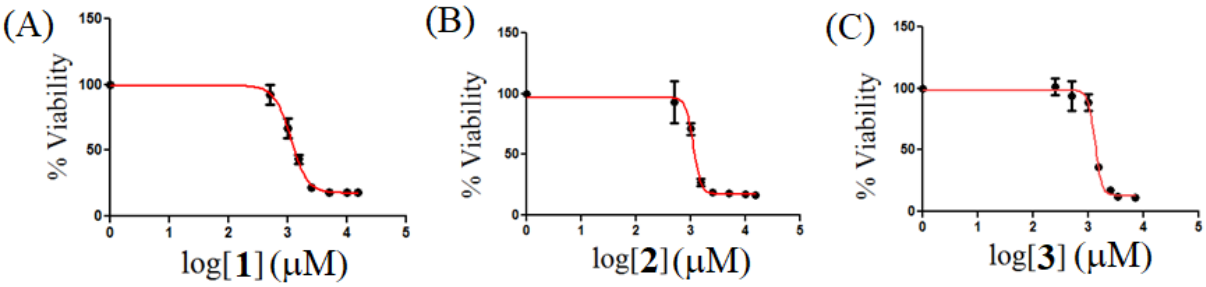

Fig. S44 Plots of cell viability (%) vs. log of concentrations of **1**-**3** against MIA PaCa-2 cell line after incubation for 48 h determined from MTT assays under normoxic condition. The plots provided are for one independent experiment (each concentration in triplicate) out of at least three independent experiments.

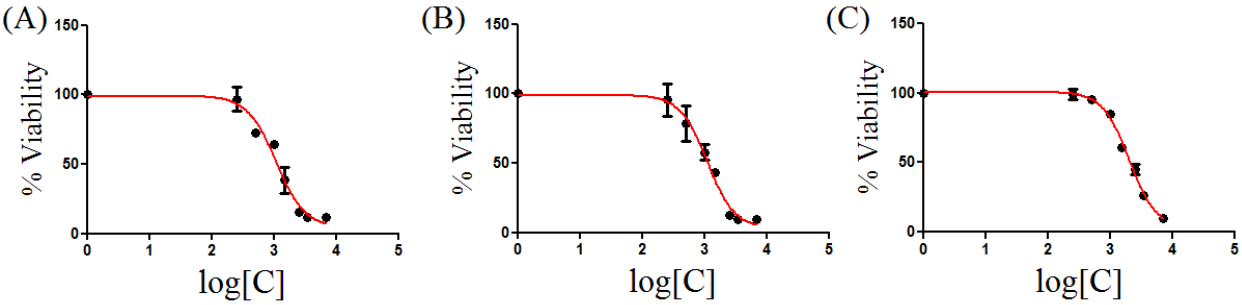

Fig. S45 Plots of cell viability (%) vs. log of concentrations of **1**-**3** against MDA-MB-231 cell line after incubation for 48 h determined from MTT assays under normoxic condition. The plots provided are for one independent experiment (each concentration in triplicate) out of at least three independent experiments.

Table S1 Cell cycle analysis of MIA PaCa-2 treated with **1-3**, showing percentage of arrest in different phases of cell cycle.

	Sub G1	G0/G1	S	G2/M
DMSO Control	0.11	59.26	15.33	25.73
1 (0.5µM)	0.97	64.38	11.12	23.58
1 (1.0µM)	0.93	68.31	11.31	19.57
2 (0.5µM)	1.44	66.88	11.61	20.28
2 (1.0µM)	0.79	68.89	10.87	19.67
3 (0.5µM)	2.49	63.89	11.80	22.22
3 (1.0µM)	1.1	70.51	11.11	17.34

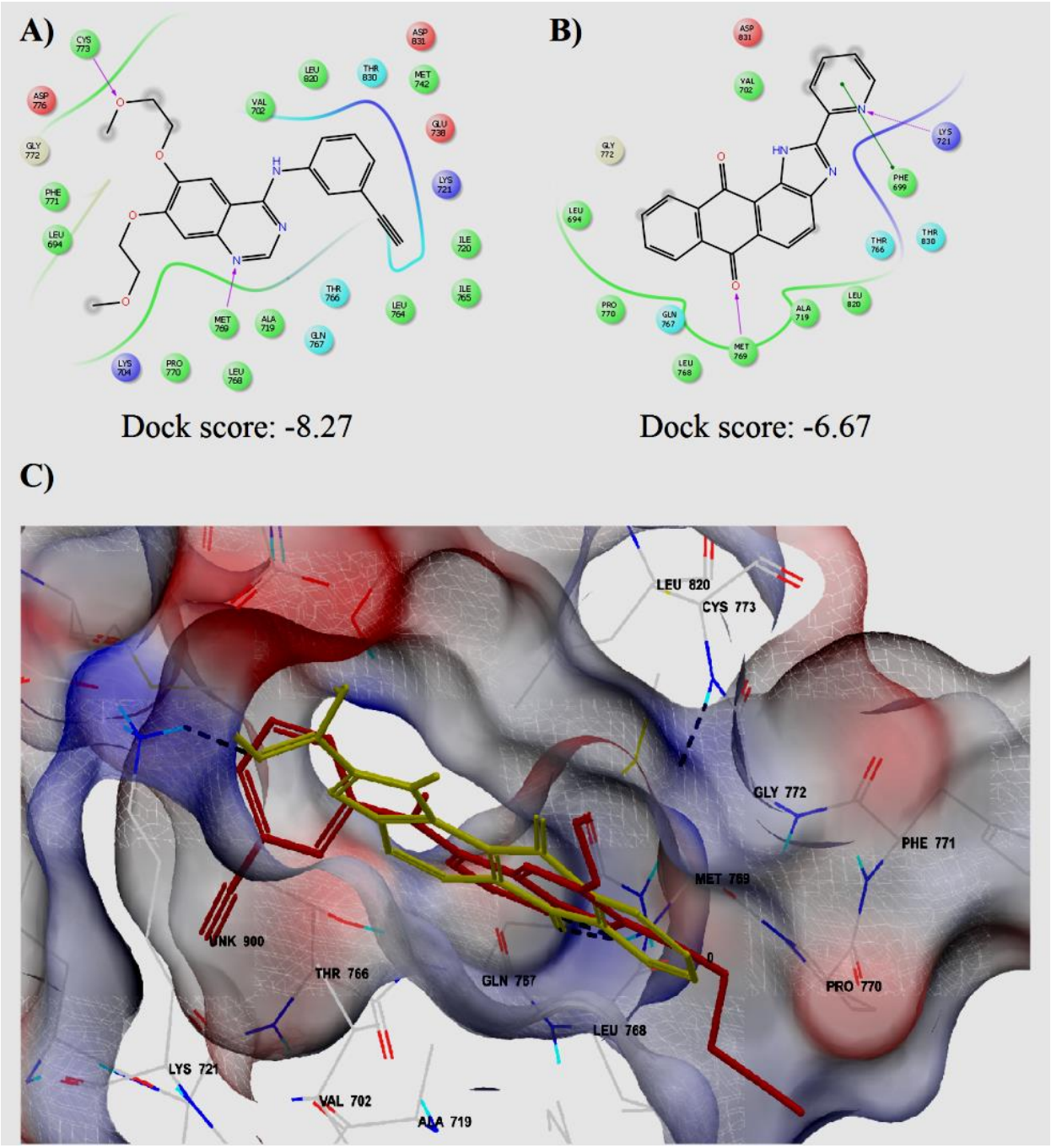

Fig. S46 EFGR kinase domain (PDB: 1M17) interaction of the clinical EGFR inhibitor Erlotinib (A) vs. the PAIDH ligand (B) using Schrödinger. (C) A representative diagram of both Erlotinib and PAIDH at the active sight cavity of the 1M17 protein showing both of them occupy almost the same site but the PAIDH shows a pi-pi stacking with phenylalanine (Phe 699) from the active. Yellow: PAIDH, Red: Erlotinib.

References:

1. J. Stamos, M. X. Sliwkowski, C. Eigenbrot, *J Biol Chem* 2002**, 277**, 46265-46272.
2. S. Bhattacharyya, K. Purkait, A. Mukherjee, *Dalton Trans.* 2017, **46**, 8539-8554.
3. A. L. Hopkins, J. Ren, R. M. Esnouf, B. E. Willcox, E. Y. Jones, C. Ross, T. Miyasaka, R. T. Walker, H. Tanaka, *J. Med. Chem.* 1996, **39**, 1589-600.
4. W. L. Jorgensen, D. S. Maxwell, J. Tirado-Rives, *J. Am. Chem. Soc.* 1996, 118, 11225-11236.
5. S. Ganguly, B. Debnath, *Medicinal Chemistry* 2014, **4**, 558-568.